

ANALYTICAL STUDY ON PERMORMANCE OF BASAL REINFORCED PILED EMBANKMENT

A DISSERTATION

SUBMITTED IN PARTIAL FULLFILLMENT OF THE REQUIREMENTS FOR
THE AWARD OF THE DEGREE

OF

MASTER OF TECNHNOLGY

IN

GEOTECHNICAL ENGINEERING

Submitted by:

JEEVISH JINDAL

2K23/GTE/04

Under the supervision of

Prof. RAJU SARKAR



DEPARTMENT OF CIVIL ENGINEERING

DELHI TECHNOLOGICAL UNIVERSITY

(Formerly Delhi College of Engineering)

Bawana Road, Delhi-110042

MAY, 2025

ANALYTICAL STUDY ON PERMORMANCE OF BASAL REINFORCED PILED EMBANKMENT

A DISSERTATION

SUBMITTED IN PARTIAL FULLFILLMENT OF THE REQUIREMENTS FOR
THE AWARD OF THE DEGREE

OF

MASTER OF TECNHNOLGY

IN

GEOTECHNICAL ENGINEERING

Submitted by:

JEEVISH JINDAL

2K23/GTE/04

Under the supervision of

Prof. RAJU SARKAR



DEPARTMENT OF CIVIL ENGINEERING

DELHI TECHNOLOGICAL UNIVERSITY

(Formerly Delhi College of Engineering)

Bawana Road, Delhi-110042

MAY, 2025

DELHI TECHNOLOGICAL UNIVERSITY
(Formerly Delhi College of Engineering)
Bawana Road, Delhi-110042

CANDIDATE'S DECLARATION

I, JEEVISH JINDAL, 2K23/GTE/04, student of MTech (Geotechnical Engineering), hereby declare that the project Dissertation titled “Analytical Study of Performance of Basal Reinforced Piled Embankment” which is submitted by me to the Department of Civil Engineering, Delhi Technological University, Delhi in partial fulfilment of the requirement for the award of the degree of Master of Technology, is original and not copied from any source without proper citation. This work has not previously formed the basis of any Degree, Diploma Associateship, Fellowship or other similar title or recognition.

Place: Delhi

JEEVISH JINDAL

Date: 28 May, 2025

DEPARTMENT OF CIVIL ENGINEERING

DELHI TECHNOLOGICAL UNIVERSITY

(Formerly Delhi College of Engineering)

Bawana Road, Delhi-110042

CERTIFICATE

I hereby certify that the Project Dissertation titled “Analytical Study of Performance of Basal Reinforced Piled Embankment” which is submitted by Jeevish Jindal, 2K23/GTE/04, Department of Civil Engineering, Delhi Technological University, Delhi in a partial fulfilment of the requirement for the award of the degree of Master of Technology, is a record of the project work carried out by the student under my supervision. To the best of my knowledge this work has not been submitted in part or full for any Degree or Diploma to this University or elsewhere.

Place: Delhi

Date: 28 May, 2025

Prof. RAJUSARKAR

SUPERVISOR

ABSTRACT

Due to severe settlement, low capacity for bearing, and stability over time problems, soft subsoils make embankment construction difficult. Basal Reinforced Piled Embankments (BRPEs) are a reliable ground enhancement method for these difficulties. This approach uses vertical piles and geosynthetic support at the embankment's base to transfer loads and reduce settling. This study employs PLAXIS 2D, a geotechnical engineering finite element software, to evaluate BRPE systems on soft subsoils.

The project involves modelling a basal-reinforced piled embankment over soft clay in 2D. The analysis examines how pile spacing, reinforcing rigidity, embankment height, and the pile cap size affect load transfer, settling behaviour, and arching mechanisms. The Weak Soil Creep model captures main and secondary consolidating effects in soft subsoil, while geogrid elements represent reinforcement.

Results show basal reinforcement considerably improves embankment performance. It improves pile load distribution and decreases overall and differential settlements. Geosynthetic membranes, especially at shorter pile spacings and greater stiffness, improve soil arching while decreasing soft ground stress. System reliability and efficiency depend on embankment elevation and the pile cap size.

This study emphasises the need of optimising BRPE system design factors and offers soft soil experts' practical advice. The findings suggest PLAXIS 2D can reliably model complicated ground-structure interactions and drive future engineering and field validation.

DEPARTMENT OF CIVIL ENGINEERING

DELHI TECHNOLOGICAL UNIVERSITY

(Formerly Delhi College of Engineering)

Bawana Road, Delhi-110042

ACKNOWLEDGEMENT

The following research work is the final output of my two years master's degree in Geotechnical Engineering at the Delhi Technological University (DTU), New Delhi, India. I would like to express my heartfelt appreciation to the staff of Delhi Technological University (DTU) for their prompt academic and administrative support, without which this work would not have been successful.

I am grateful to my thesis supervisor, Prof. Raju Sarkar for his valuable guidance and constructive scholarly suggestions during the planning and implementation of my project work. Without his timely inputs and periodic assessments, this project would not have given the desired results. I would also like to thank my friends in the college throughout the study program with whom I gained valuable experiences through which I tried to dive into the deep sea of knowledge.

Place: Delhi

JEEVISH JINDAL

Date: 28 MAY 2025

Table of Contents

CANDIDATE’S DECLARATION	ii
CERTIFICATE.....	iii
ABSTRACT	iv
ACKNOWLEDGEMENT	v
LIST OF TABLES	viii
LIST OF FIGURES.....	ix
LIST OF SYMBOLS AND ABBREVIATIONS.....	x
CHAPTER 1 INTRODUCTION.....	1
1.1 BACKGROUND AND MOTIVATION	1
1.2 PROBLEM STATEMENT	2
1.3 LOCATION OF SOFT SUBSOILS IN INDIA.....	3
1.4 CASE STUDIES.....	5
1.4.1 Visvesvaraya Setu (Okhla Flyover) Project	5
1.4.2 Road Over Bridge near PIVIC Building, Port Road, Mundra, Gujarat	7
1.4.3 Visakhapatnam Port Connectivity Road Project, Andhra Pradesh.....	9
1.5 OBJECTIVES OF STUDY	10
1.6 ORGANISATION OF DISSERTATION	11
CHAPTER 2 LITERATURE WORK	12
2.1 LITERATURE REVIEW	12
2.2 GAPS IN RESEARCH	15
CHAPTER 3 METHODOLOGY	16
3.1 MATERIALS USED	16
3.2 LABORATORY TESTING AND EXPERIMENTAL STUDIES.....	17
3.2.1 Proctor Compaction Test.....	17
3.2.2 Atterberg Limits Test	19
3.2.3 Direct Shear Test	21
3.3 MATERIAL PARAMETERS	27
3.4 NUMERICAL MODELLING	27
3.4.1 PLAXIS 2D MODEL.....	28
3.4.2 MODEL DETAILS.....	28

CHAPTER 4 RESULTS AND DISCUSSIONS.....	30
4.1 INFLUENCE OF GEOGRID TENSILE STRENGTH AND ANCHORAGE LENGTH ON SAR.....	30
4.2 INFLUENCE OF PILE SPACING AND GEOGRID TENSILE STRENGTH ON SAR.....	31
4.3 INFLUENCE OF PATTERN OF PILES ON SAR.....	33
4.4 INFLUENCE OF NO OF CYCLIC LOADING ON SETTLEMENT.....	34
4.5 COMPARISON OF RESULTS WITH AND WITHOUT BASAL REINFORCEMENT	35
4.5.1 Without Basal Reinforcement	35
4.5.2 With Basal Reinforcement.....	39
CHAPTER 5 CONCLUSIONS	42
5.1 OPTIMAL TENSILE STRENGTH AND PILE SPACING RELATIONSHIP.....	42
5.2 ANCHORAGE LENGTH REQUIREMENT.....	42
5.3 PERFORMANCE UNDER CYCLIC LOADING AND SETTLEMENT BEHAVIOUR.....	43
5.4 PILE ARRANGMENT GEOMETRY AND LOAD DISTRIBUTION.....	43
5.5 COST EFFICENCY THROUGH REINFORCEMENT THROUGH REINFORCEMENT OPTIMISATION	44
5.6 FINAL REMARKS	44
APPENDIX-1	45
Product Data Sheet- Biaxial Geogrid SQ 2525	45
References	46

LIST OF TABLES

Table 1.1 Geotechnical Properties of Soft Clays from Different Parts of India.....	4
Table 1.2 Classification of Soft Soils Based on Shear Strength.....	5
Table 3.1 Observation Table for Proctor Compaction Test (Subsoil Sample).....	17
Table 3.2 Observation Table for Proctor Compaction Test (Granular Fill Sample).....	18
Table 3.3 Observation Table for Atterberg Limit Tests (for Subsoil Clayey Sample)..	20
Table 3.4 Observation Table for Direct Shear Test (Granular Fill Sample)	22
Table 3.5 c and Φ values for granular fill sample.....	23
Table 3.6 Direct Shear Test Results for Granular Fill Sample	24
Table 3.7 Observation Table for Direct Shear Test (Subsoil Sample).....	24
Table 3.8 c and Φ values for subsoil sample	26
Table 3.9 Direct Shear Test Results for Subsoil Sample	26
Table 3.10 Parameters of subsoil and granular fill material samples	27
Table 3.11 Parameters of geogrid material used (Reference: Appendix-1).....	27

LIST OF FIGURES

Figure 1.1 A Basal Reinforced Piled Embankment	2
Figure 1.2 Proposed Model for embankment on Soft Clayey Subsoil	3
Figure 1.3 Spreading Geogrid as Basal Reinforcement at Okhla.....	6
Figure 1.4 Typical cross-section of the Basal Reinforcement Scheme Provided Under Reinforced Fly Ash Embankment in Okhla.....	7
Figure 1.5 Geotextile as Basal Reinforcement at Visakhapatnam.....	10
Figure 3.1 Proctor Compaction Curve for Subsoil Sample	18
Figure 3.2 Proctor Compaction Curve for Granular Fill Sample	19
Figure 3.3 Subsoil Clayey Sample represented on plasticity chart	21
Figure 3.4 Mohr-Coulomb Failure Envelope (for granular fill sample).....	23
Figure 3.5 Stress-Strain Curve for Granular Fill Sample	24
Figure 3.6 Mohr-Coulomb Failure Envelope (for subsoil sample)	25
Figure 3.7 Stress-Strain Curve for Subsoil Sample.....	26
Figure 3.8 Plaxis-2D Model of Basal Reinforced Piled Embankment System.....	28
Figure 4.1 Variation of SAR with geogrid anchorage length	31
Figure 4.2 Variation of SAR with Pile Spacing.....	32
Figure 4.3 Variation of Height of Embankment vs SAR.....	34
Figure 4.4 Variation of Settlement with number of cycles	35
Figure 4.5 Excess Pore Water Pressure dissipation with time.....	37
Figure 4.6 Excess Pore Water Pressure vs Time Plot near the middle and at the toe...	37
Figure 4.7 Deformation in mesh with time	38
Figure 4.8 Displacement vs Time at the toe and near the middle.....	38
Figure 4.9 Deformed mesh (with Basal Reinforcement).....	40
Figure 4.10 Displacements with time (with Basal Reinforcement)	40
Figure 4.11 Displacements vs Time (with Basal Reinforcement)	41
Figure 4. 12 Excess Pore Water Pressure dissipation with basal reinforcement	41

LIST OF SYMBOLS AND ABBREVIATIONS

Abbreviations/Symbols	Description
w_L	Liquid Limit
W_p	Plastic Limit
I_p	Plasticity Index
C_c	Coefficient of Compression
C_v	Coefficient of Consolidation
E_i	Initial Tangent Modulus
E_{50}	Secant Modulus
e_0	Natural Void Ratio
e	Void Ratio
c	Cohesion
Φ	Friction Angle
γ	Unit Weight
γ_b	Bulk Unit Weight
γ_d	Dry Unit Weight
w	Water Content
E	Modulus of Elasticity
μ	Poisson's Ratio
MD	Machine Direction
XMD	Perpendicular to Machine Direction
T	Tensile Strength
ROB	Road Over Bridge
CH	High Compressible Clay
P.R.	Proving Ring
DST	Direct Shear Test
SAR	Soil Anchorage Ratio

CHAPTER 1

INTRODUCTION

1.1 BACKGROUND AND MOTIVATION

Embankments are essential for the development of roadways, railways, and flood control infrastructure. The subsoil significantly influences the stability and efficacy of these structures. Embankments are more prone to failure and settlement over soft clay soils, such as those found in coastal regions, riverbanks, and reclaimed land. Soft clays present geotechnical challenges because to their low shear strength, high water content, low permeability, and extended consolidation durations.

Practicing engineers are utilising various ground improvement techniques to securely construct banks on soft subsoils, including a partial or complete replacement of soft subsoil with soil exhibiting enhanced load-bearing properties, phased construction of the embankment, demanding stabilisation of subsoil using admixtures such as lime columns, and the setting up of prefabricated vertical drains with preloading. Utilisation of stone columns to improve the load-bearing capacity of soft subsoil. The utilisation of reinforcing elements, whether metal or polymerised, at the fundamental level and above Incorporation of the previously listed factors. The staged construction of embankments is either time-consuming or uneconomical for projects with excessively soft subsurface. In these instances, piles are utilised to reinforce the embankment in alignment with the project timeline. Nevertheless, the pliable soil between the piles remains compromised; so, we employ reinforcing at the apex of the piles to facilitate the transfer of the embankment load onto the foundations.

Basal reinforcement—utilizing geosynthetic materials such as geogrids or geotextiles near the base of the embankment—can address these challenges. These materials mitigate differential settlement, transmit loads uniformly, and maintain the embankment through tightened membranes movement and soil arching. Basal reinforcement typically functions effectively with vertical elements such as piles or stone columns; however, it can also enhance performance alone. Effective and economical design necessitates comprehension of fundamental reinforcement behaviour under varying loading and soil conditions. Advanced computer methods, such as

PLAXIS 2D, facilitate the analysis of soil-structure interaction and evaluate reinforced banks in three dimensions. This research employs PLAXIS 2D to analyse basal reinforced embankments situated on soft clay soils.

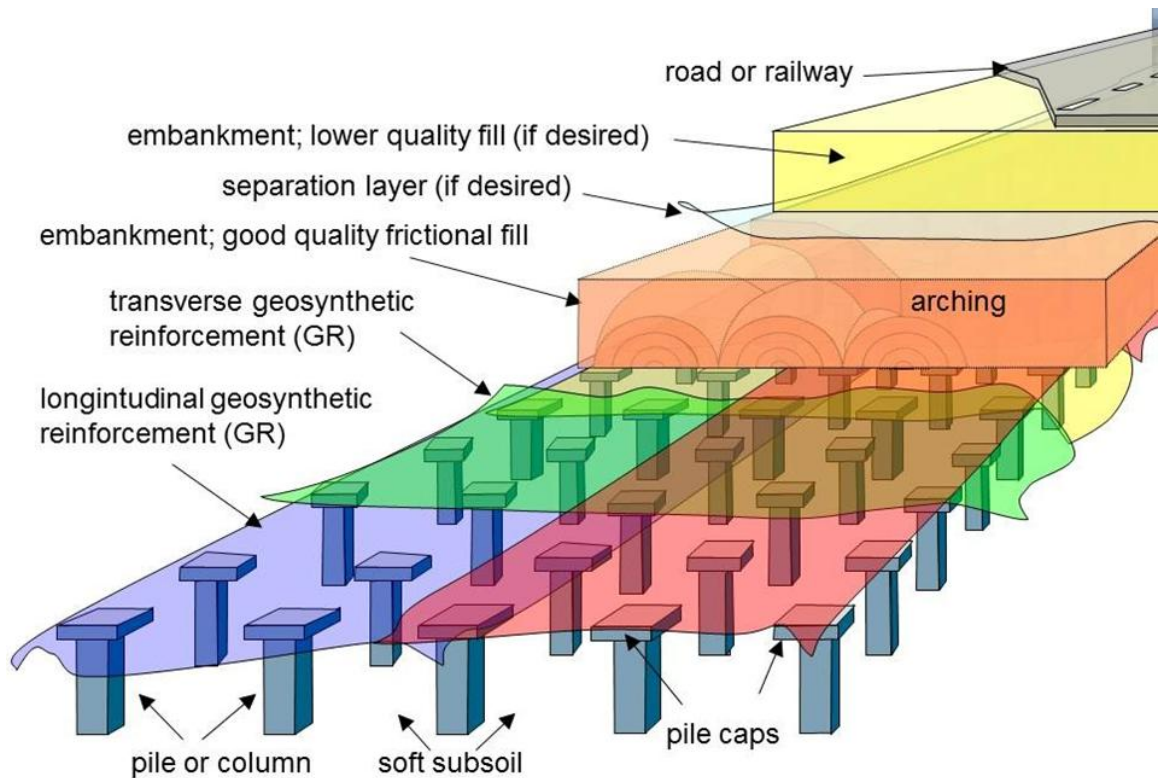


Figure 1.1 A Basal Reinforced Piled Embankment

1.2 PROBLEM STATEMENT

Soft clay foundations are very bad since they can't hold much weight and might settle unevenly and heavily when they are loaded from the outside. If you build embankments on soils like this without the right support, they could shear, deform too much, or even collapse. Basal reinforcement has showed a lot of promise in solving these problems, but the complicated relationships between the reinforcement, the embankment fill, and the soft subsoil are not always clear.

Design choices, like the kind and stiffness of the reinforcement, the height of the embankment, and the qualities of the foundation, can have a big effect on how well the whole system works. Even though geosynthetics are being used more and more in the embankment design, there is still a need for more in-depth analytical studies that look

at the full spectrum of factors that can affect them in real-life three-dimensional situations. A lot of the time, designers make simplistic assumptions that do not always show how reinforced embankments behave on soft soils.

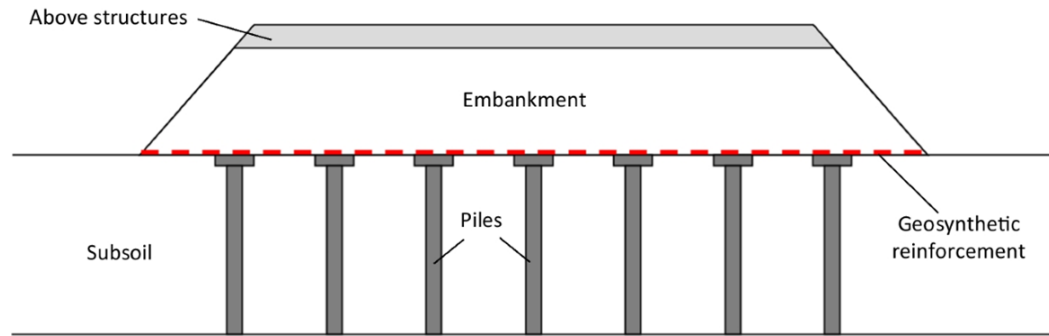


Figure 1.2 Proposed Model for embankment on Soft Clayey Subsoil

1.3 LOCATION OF SOFT SUBSOILS IN INDIA

India has a huge and varied geography that includes many different types of soil. Geotechnical engineers are especially concerned with soft subsoils, such as delicate marine clays and the alluvial silts. These soft soils are usually found in low-lying areas around the coast, such as river deltas and flood plains, where organic sedimentation has built up thick, weak soil deposits over hundreds of years. Their engineering behaviour, which includes poor shear strength, high compressibility, and low permeability, makes them very hard to build with, particularly when it involves load-bearing structures like embankments.

The eastern coastal belt, which goes from West Bengal through Odisha and Andhra Pradesh to Tamil Nadu, is one of the most well-known areas in India having a lot of soft soil. The Sundarbans delta area in West Bengal, for example, is mostly made up of vast layers of soft clay and silt that were left behind by the Ganges, Brahmaputra, and Meghna River systems. This area often has challenges like settling foundations and unstable slopes, which makes it a great place for researchers to study ground repair methods like basal reinforcement.

The Chennai coastline region, which is located to the south, is another important place where soft marine clays are often found. The demand for solid ground improvement methods in this area has become urgent because of the increasing growth

of cities and the expansion of infrastructure, including roads, metro lines, and port facilities. Ground stabilisation and reinforcing procedures have been used a lot on projects like the Chennai Metro Rail to deal with deep soft soil deposits.

The Krishna-Godavari delta in Andhra Pradesh is another well-known example of soft soil topography, with sediments that are silty and clayey. This deltaic area is very important for farming and the economy, but it also floods often and gets waterlogged in the winter, which makes the subsoil even weaker. Building embankments in these places is often necessary for flood protection and transportation infrastructure. Using base reinforced embankments is extremely important to make sure they stay stable over time.

Soft marine clays can also be found on the western coast, especially in places like Mumbai and the Gulf of Khambhat in Gujarat. In Mumbai, massive land reclamation for urban growth has created a pressing need for new geotechnical solutions to deal with concerns with settlement and bearing capacity. For instance, the Mumbai Coastal Road Project requires a lot of geotechnical design to deal with the poor soils.

Table 1.1 Geotechnical Properties of Soft Clays from Different Parts of India [1]

Properties	Mumbai	Outer Harbour Visakhapatnam	Kandla Port Kandla	Wellington Island Cochin	Ran of Kutch
Depth of Soft Clay, m	1.0-2.0	12.0-18.0	12.0-20.0	21.0-28.0	3.0-17.0
Physical Properties					
Liquid Limit, w_L %	30-144	65-97	55-80	105-120	43-73
Plastic Limit, w_P %	18-55	40-45	20-35	40-45	18-45
Natural Moisture Content, w %	40-139	80-90	35-75	65-102	40-80
Plasticity Index I_p	15-89	24-55	20-50	65-75	18-45
Specific Gravity	2.32-2.88	2.65	2.72	2.53-2.60	2.61-2.78
Clay Content	54-100	40-70	30-35	50-65	10-47
Engineering Properties					
Undrained Shear Strength kN/m^2	15-45	20-40	17-35	5-15	5-20
Natural Void Ratio, e_0	1.96-2.81	2.47-2.57	1.1-1.5	2.18-2.30	1.5-2.0
Compression Index	0.37-1.32	0.82-0.88	0.3-0.55	0.65-0.90	0.30-0.56
Coefficient of Consolidation, cm^2/sec	1.23×10^{-4}	1.06×10^{-4}	8.8×10^{-4}	2.54×10^{-4}	

Fine Grained soil are classified on the basis of undrained shear strength as ranging from very soft to hard, as shown in Table 1.2. A broad correlation between the undrained shear strength with SPT and SCPT is also included in the Table. The use of basal reinforcement is most advantageous where soft to very soft soils with undrained shear strength about 50 kPa and less are present.

Table 1.2 Classification of Soft Soils Based on Shear Strength [1]

Consistency	Unconfined Compressive Strength (kPa)	SPT Value (N)	SCPT Value (kPa)
Hard	>400	>30	>6000
Very Stiff	200-400	15-30	3000-6000
Stiff	100-200	8-15	1600-3000
Medium	50-100	4-8	800-1600
Soft	25-50	2-4	400-800
Very Soft	<25	0-2	0-400

For this study, it's important to know where soft subsoils are found in India so that we can find places where basal reinforcement techniques will work well. As the need for transportation and flood-resistant infrastructure grows in these soft soil areas, studies like this can help us figure out how to build safe, effective, and affordable embankments utilising cutting-edge tools like PLAXIS 2D. Knowing where soft subsoils exist helps with improved planning, site inspection, and the use of ground improvement methods that are most suited to India's particular geotechnical circumstances.

1.4 CASE STUDIES

1.4.1 Visvesvaraya Setu (Okhla Flyover) Project

The Delhi Public Works Department, in collaboration with the Central Road Research Institute, erected a strengthened fly Ash approaches embankment alongside the slip roads adjacent to NH-2 at Okhla, Delhi. During the design phase, it was observed that the safe bearing capacity of the subsoil was about 125 kN/m², whereas the bearing pressure exerted by the reinforced fly Ash embankment walls was around 193 kN/m².

Ground enhancement was executed utilising a pair of bi-oriented geogrids at depths of 0.45 m and 1.0 m, positioned at the base of the strengthened fly ash embankment. Bottom ash, a byproduct of thermal power plants, was utilised as friction fill in the basal reinforcement section. Bottom ash was deposited in two layers, reaching an elevation of 0.5 meters. Every layer was crushed to 95% of Proctor density. A bi-oriented geogrid was deployed over the compressed fill. Rods having a diameter of 10 mm were secured to guarantee the geogrid remained in position. Compaction was executed using an 8-ton static roller, succeeded by a vibrating roller. The flyover was inaugurated for traffic in January 1996, and has been functioning effectively.



Figure 1.3 Spreading Geogrid as Basal Reinforcement at Okhla [1]

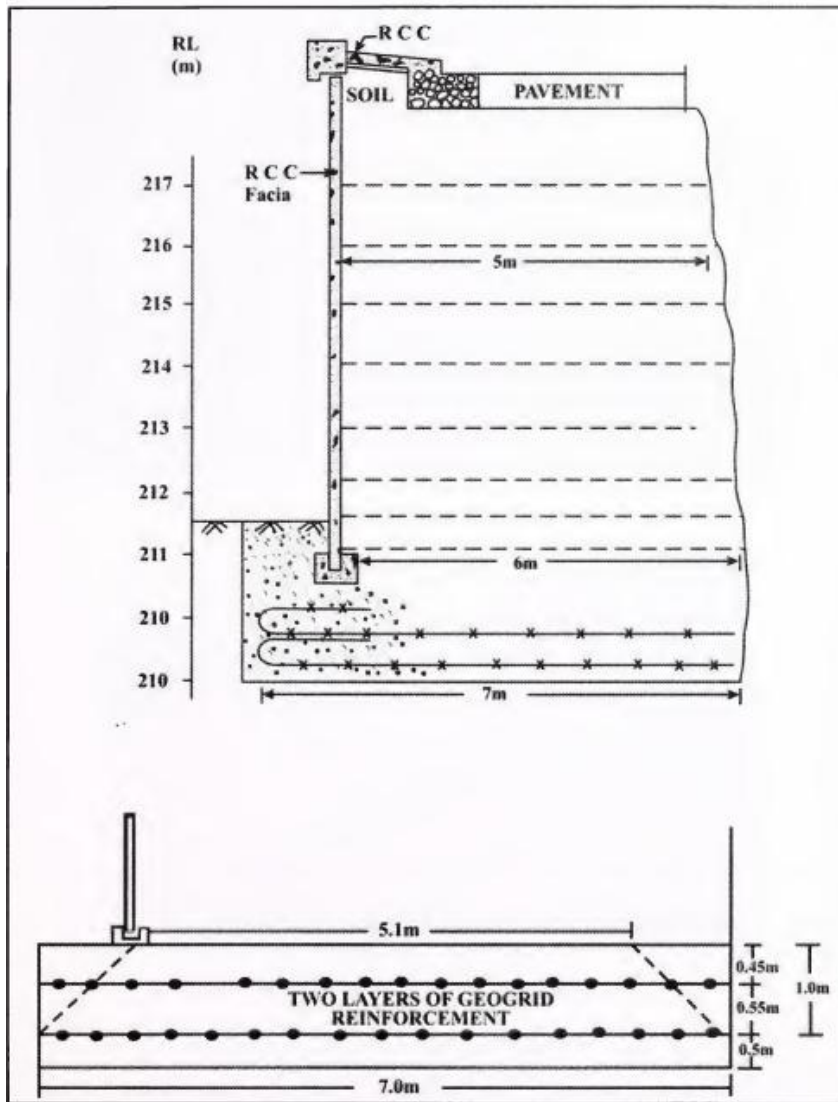


Figure 1.4 Typical cross-section of the Basal Reinforcement Scheme Provided Under Reinforced Fly Ash Embankment in Okhla [1]

1.4.2 Road Over Bridge near PIVIC Building, Port Road, Mundra, Gujarat

The Mundra Special Economic Zone (SEZ) is situated in the Kutch District of Gujarat. This is connected to the National Highway Network via an extension of NH 8A Ext. from Mundra-Anjar-Bhimasar. A railway intersects the port connecting road (Mundra to NH 8A). A ROB (8 lane) was designed to traverse the railway line. The methodologies of ROB were suggested to be preserved with an enhanced soil wall. Granular fill dirt - unit weight 20 kN/m^3 , angle of internal friction (ϕ) = 32° . The maximum height of the reinforced soil wall was 9 meters. The soil consisted of clayey silt to a depth of 3.0 m, followed by sand with silt extending to 4.5 m depth. This is

supported by sandy silt containing traces of clay up to a depth of 9.0 meters. The groundwater table was located at a depth of 1.5 meters. High-strength geogrids featuring a mono-axial arrangement of geosynthetic strips with a planar configuration were employed as basal reinforcement to enhance the strength of the underlying soil, accompanied by a drainage layer and a geotextile interposed between them.

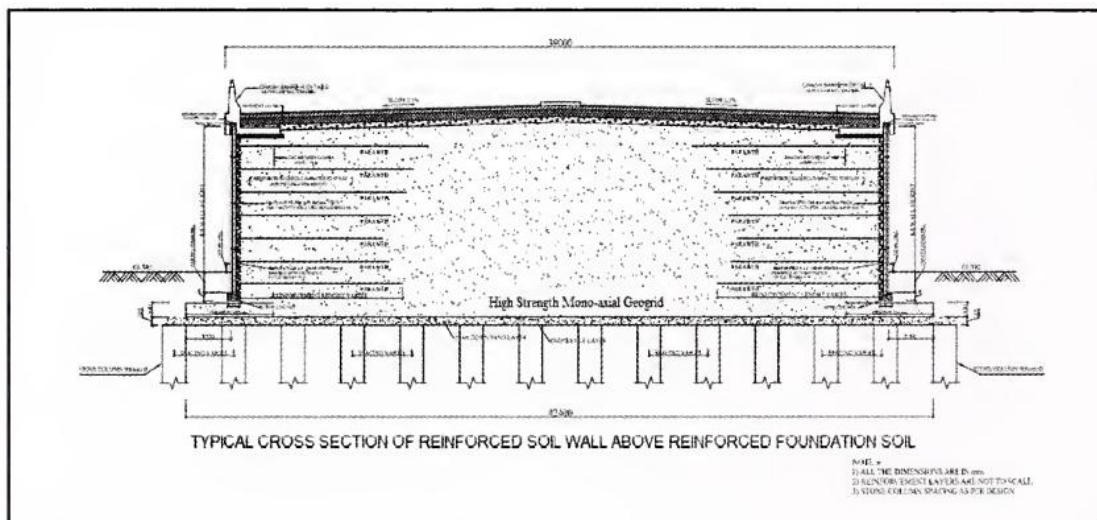




Figure 1.6 Installation of Bonded Geogrid, Mundra, Gujarat

1.4.3 Visakhapatnam Port Connectivity Road Project, Andhra Pradesh

The NHAI, in collaboration with the Visakhapatnam Port Trust, has created a new route to facilitate rapid and convenient access to Visakhapatnam port from NH-5. The project road was around 12.3 km, of which 4.567 km underwent ground enhancement utilising prefabricated vertical drains and a high-strength geotextile basal reinforcement layer. The soft coastal clay exhibited a thickness of 10 to 18 meters, with an undrained shear strength ranging from 5 to 8 kPa. C_u fluctuated between 0.8 and 1.2. According to the IS categorisation system, the soil was categorised as CH type. The embankment's height ranged from 2.5 to 3.2 meters. The embankment construction involved the installation of a working platform with a thickness of 0.7 m over the original ground. Prefabricated Vertical Drains were constructed at 1.15 m center-to-center in a triangle configuration following the placement of the initial embankment. A sand drainage layer with a thickness of 0.6 meters was subsequently placed over the initial embankment. A high-strength polymeric woven geotextile was then deployed over the sand drainage layer. The geotextile employed exhibited a design tensile strength of 230 kN/m. The geotextile was secured at the ends with sand-filled sacks. The embankment construction was executed in two phases: 1.75 m for the first phase and 2.0 m for the second phase. The duration for each phase was 175 days. Approximately

124,000 square meters of geotextile were utilised in this project as a reinforcement layer. The project was finished and opened to traffic in 2007.



Figure 1.5 Geotextile as Basal Reinforcement at Visakhapatnam

1.5 OBJECTIVES OF STUDY

The primary aim of this study is to evaluate the efficacy of basal reinforcement in embankments built on soft clay substrates utilising PLAXIS 2D. Defined objectives encompass:

- i. To examine the load distribution mechanism and stress transmission from the embankment to the soft subsurface.
- ii. To assess the effect of geosynthetic reinforcement in mitigating total and differential settlement.
- iii. To find the influence of Geogrid tensile Strength and anchorage length on SAR
- iv. To find the Influence of Pile Spacing and Geogrid Tensile strength on SAR
- v. To find influence of Patten of Piles on SAR

1.6 ORGANISATION OF DISSERTATION

This document is structured into five chapters along with an appendix, each serving a specific role in presenting the research comprehensively.

Chapter 1: Introduction outlines the background and motivation for the study, emphasizing the need for efficient ground improvement techniques over soft soils. It reviews several relevant case studies from different parts of country, offering insight into practical challenges and solutions. The objectives of the research are clearly defined to guide the study's direction.

Chapter 2: Literature Review presents an overview of previous research on geosynthetic-reinforced pile-supported embankments. It critically examines existing methodologies and findings, identifying key research gaps that this study aims to address.

Chapter 3: Methodology describes the numerical analysis procedures used in the study. It details the model setup, material properties, boundary conditions, and the software tools employed. This chapter establishes the analytical framework used to simulate the behaviour of the reinforced embankment system.

Chapter 4: Results and Discussion presents the outcomes of the simulations. It analyses the effects of parameters such as pile spacing, geogrid tensile strength, and anchorage length on the soil arching ratio and settlement behaviour. These results are interpreted with reference to both the study objectives and existing literature.

Chapter 5: Conclusions and Final Remarks summarizes the key findings, offering practical insights and design recommendations. It also suggests areas for future research to build upon the current work.

Appendix-A: The appendix provides supplementary information that supports the main content of the thesis.

CHAPTER 2

LITERATURE WORK

2.1 LITERATURE REVIEW

The optimal design of piled embankments with basal reinforcement can be achieved by optimizing the design parameters, such as geosynthetic strength, geosynthetic thickness, and bearing capacity, to reduce construction costs. [2] Attaching anchors to geogrid significantly enhances shear resistance to failure, with increased normal pressure and anchor size. [3] Anchored geogrid reinforcements can significantly increase shear strength and reduce volumetric dilation, while non-anchored geogrid reinforcements can enhance peak shear strength. [4] Geocomposite and geogrid significantly enhance load-penetration responses in soil-aggregate systems, improving functionalities of reinforcing materials. [5]

Geogrid-soil interaction is influenced by geogrid aperture size, tensile stiffness, geogrid type, and reinforcement configurations, with the most effective load transfer achieved using closely spaced transverse members at each rib. [6] Geogrid-reinforced soil increases foundation bearing capacity by up to 635%, with optimal aperture size being 4 times soil grain size and footing width being 13-25 times soil grain size. [7] (Gh. Tavakoli Mehrjardi et al.) The highest interface shear strength is achieved at 45° shear direction, with increasing anisotropy of biaxial geogrid decreasing overall strength and affecting geogrid rib passive resistance. [8] The study developed a new equation to predict the bearing capacity of geogrid-reinforced sand, with a constant strain value at 0.5B embedment depth and a significant effect of shorter geogrid length layers. [9]

Geogrid reinforcement enhances soil strength, with increased layers enhancing subgrade modulus and a new method proposed for determining an approximate value of subgrade reaction modulus in reinforced soils. [10]. This study simulated pile-soil-pile interaction in battered pile groups using finite element analysis, examining the effects of batter angle, slenderness ratio, spacing between piles, and pile-soil stiffness ratio on interaction factors. [11] Group efficiency of helical piles in soft clay soil is significantly influenced by the number of piles, center-to-center spacing, and assumed failure criteria.

[12] The load pattern and Poisson's ratio effect greatly influence the pullout performance of anchor bolts in pipe piles, with anchorage-beam tests providing more sensible results for anchor bolt design. [13] The study demonstrates that sloping ground significantly affects the capacity and lateral deflection behaviour of group of piles in soft to medium-stiff clay and silt soils. [14]

Y. Zhuang et al [15] told that Cyclic loading increases maximum settlement at the base of the embankment by 23-55%, while unloading slightly rebounds the reduction in efficiency. Increasing the number of cyclic loading cycles improves arching of the soil and reduces surface settlement in reinforced piled embankments. [16]

Geosynthetic-reinforced and pile-supported embankments perform well when considering the interaction between soil, geosynthetics, pile, and subsoil, but their load efficacy and differential settlement predictions vary greatly among design methods. [17]. Two geosynthetic reinforcement layers with a fill layer in between reduce surface settlement and tensile forces, improving soil arching stability under cyclic loading in geosynthetic-reinforced pile supported embankments. [18] Geogrid reinforcement placed directly on top of soft clay layers may not significantly contribute to embankment stability due to poor adhesion at the clay-reinforcement interface. [19]

Subsoil can carry as much as 75% of the arching embankment load in reinforced piled embankments, with geogrid playing a significant role in load transfer, but may lead to intolerable geogrid strain due to large setbacks for the present standard model (pile spacing of 2.5 m, geogrid stiffness of 6 MN/m, embankment height of 6 m, and subsoil compression index of 0.7). Also, the proportion is much larger for the lower value of pile spacing, geogrid stiffness, embankment height, and subsoil compression index. The maximum settlement of subsoil is found to be more sensitive to the pile spacing than to the geogrid stiffness. The theoretical method shows reasonable agreement with the FE results and can therefore be used to predict the effect of subsoil in reinforced piled embankments. The geogrid has a significant role in carrying the entire embankment load without the subsoil support. However, this effect may lead to intolerable geogrid strain due to relatively large settlement. [20]

Ning Zhang et al. evaluated that Basal geotextile reinforcement can reduce vertical displacements of subsoil during embankment construction, but cannot increase overall safety factor. The results showed basal reinforcement cannot increase the overall factor

of safety, but the factor of safety at the local position, under reinforcement, can be increased during the construction procedure, and this is due to the confinement of the soil element by the reinforcing fabric. Thus, in these circumstances, one layer of basal geotextile reinforcement can prevent sudden failure of subsoil during embankment construction. [21]

The simplified model for reinforced piled embankments demonstrates that subsoil contributes most to overall vertical equilibrium, while reinforcement helps reduce vertical stress acting on the subsoil. [22] Using appropriate stiffness reinforcement in geosynthetic-reinforced pile-supported embankments over voids ensures the development and stability of maximum soil arching. [23]

Prefabricated vertical drains and surcharge preloading significantly shorten subsoil consolidation time and reduce post-consolidation lateral displacements and crest settlements in reinforced floating column-supported embankments. [24] Y. Zhuang et al. presented a simple design approach for geogrid-reinforced pile-supported embankments, highlighting the importance of geogrid reinforcement and underlying subsoil contributions, and provides an approximate equation of vertical equilibrium for use in design. [25] Mattress foam can simulate partial subsoil support in piled embankments, offering a cost-effective solution for transport line construction in soft soils. [26]

D. Bergado et al. told that High-strength, nonwoven geotextile as base reinforcement significantly increases the ultimate height of embankments on soft clay, improving stability and reducing rapture. [27] Progressive yielding/softening of soil-cement columns under embankment loading can cause rapid settlement rate increases, highlighting the need for continuous quality control using all-core boring and 3D finite element analysis. [28]

Geosynthetic-reinforced embankments can significantly increase embankment stability, but creep of geosynthetics can decrease failure height. [29] A 3D numerical finite difference model effectively assesses the performance of a rigid inclusion reinforced railway embankment under cyclic loading, highlighting settlements, stress distribution, and axial-flexural response. [30]

A higher embankment load is transferred to the surrounding soil when a GESG is constructed on a weaker substratum, causing larger increases in settlement and lateral

displacement. [31] The performance of reinforced pile-supported embankments on soft soil can be improved by varying the embedded length, diameter, and elastic modulus of the piles. [32]

V. Vignesh et al. suggested that Group efficiency of helical piles in soft clay soil is significantly influenced by the number of piles, center-to-center spacing, and assumed failure criteria. [33] The maximum allowed centre-to-centre distance between piles in lightly piled embankments can potentially be increased to 1.4 m, potentially reducing the number of piles by as much as one third. [34]

Geosynthetic reinforcement in triangular-pattern pile-supported embankments reduces soil arching but increases the total load carried by the piles, with the lower layer having a greater impact on load transfer. [35] Optimized periodic pile barriers with equilateral triangular layouts can effectively isolate elastic waves, offering extensive application prospects in engineering practice. [36]

2.2 GAPS IN RESEARCH

Although multiple studies have shown the efficacy of basal reinforcement in enhancing embankment performance on soft clay substrates, several research deficiencies persist. Many current analyses depend on two-dimensional models, which frequently do not accurately represent the complete three-dimensional in nature stress distribution and soil-structure interaction. The field assessment of numerical findings is constrained, resulting in uncertainties in practical applications. The long-term performance of geosynthetics under creep, cyclic loading, and consolidation conditions remains inadequately comprehended. There is a deficiency of thorough research investigating the synergistic impacts of reinforcement rigidity, embankment geometry, and diverse subsoil profiles under different stress conditions. Moreover, regional studies concentrating on Indian soil conditions, particularly utilising contemporary tools such as PLAXIS 2D, are limited. Rectifying these deficiencies is crucial for formulating more dependable, site-specific design protocols for embankments built on soft clay utilising basal reinforcement.

CHAPTER 3

METHODOLOGY

3.1 MATERIALS USED

In this study, two different types of soil samples have been selected and utilized for detailed laboratory analysis and subsequent numerical modelling. The primary objective of using these samples is to evaluate their behaviour and characteristics for geotechnical engineering applications using PLAXIS 2D, a finite element software widely employed in soil-structure interaction analysis.

The first soil sample that was collected and analysed is a soft subsoil. Based on a preliminary visual inspection conducted at the site, this soil was identified as clayey silt. Its texture appeared smooth and fine-grained, indicating a significant presence of silt with some clay content. Such soils typically exhibit low shear strength and high compressibility, making their behaviour under loading conditions crucial for analysis.

The second soil sample was obtained from a granular fill material that had been used in the construction of an embankment. Upon visual observation, this soil appeared to be sandy silt in nature. Granular fill materials like this generally consist of coarse particles with moderate fines, providing better drainage and higher strength properties compared to cohesive soils.

Both soil samples were subjected to a comprehensive series of laboratory tests to determine various physical and mechanical parameters essential for accurate numerical modelling. These parameters include properties such as unit weight, permeability, shear strength, stiffness, and compressibility, among others. The test results were then used as input data for the finite element model developed in PLAXIS 2D.

For the numerical analysis, the pile material has been assumed to be concrete, which is a common and reliable material in pile foundation design due to its high compressive strength and durability. Furthermore, to reinforce the soil and enhance the overall stability of the structure, a geogrid material was incorporated into the model. The specific type of geogrid used in this analytical study is Biaxial Geogrid SQ2525.

Detailed specifications and the Technical Data Sheet for this geogrid are provided in Appendix-1 of this report for reference and verification.

3.2 LABORATORY TESTING AND EXPERIMENTAL STUDIES

3.2.1 Proctor Compaction Test

Modified Proctor Test (Heavy Compaction) is conducted in the laboratory in accordance with IS 2720 (Part VIII)-1983 for both the soil samples. About 2.8 kg of oven dried soil sample was taken each and a 1000 cc mould was used in the procedure. The soil sample was sieved through set of IS Sieves and pulverized sieved samples were mixed with water thoroughly to make the moisture content about 10 % for the subsoil sample and about 8% for the granular embankment sample. The wet soil samples were compacted in three equal layers by a metal rammer weighing 4.9 kg and free fall of 45 cm with 25 uniformly distributed blows in each layer for 1000cc mould. After compacting each layer scratches were made in previous layers before placing the next layer. After compaction was completed then collar was removed from top by rotating it. Top was levelled with the straight edge and mould with soil and base plate was weighed. The test was repeated by increasing water content by 2 % in each trial. The tests were carried on till there was no decrease in weight of wet compacted soil sample in the mould.

Table 3.1 Observation Table for Proctor Compaction Test (Subsoil Sample)

Determination No.	1	2	3	4
Wt. of mould, m1, g	2028	2028	2028	2028
Wt. of mould + Compacted soil, m2, g	3908	4068	4150	4122
Wt. of compacted soil, (m2-m1), g	1880	2040	2122	2094
$\gamma_b = \frac{(m_2 - m_1)}{v_m}, g/cc$	1.88	2.04	2.12	2.09
Moisture Content, %	10.3%	13.4	17.7	21.2
$\gamma_d = \frac{100 \gamma_m}{100 + w}, g/cc$	1.70	1.80	1.80	1.73

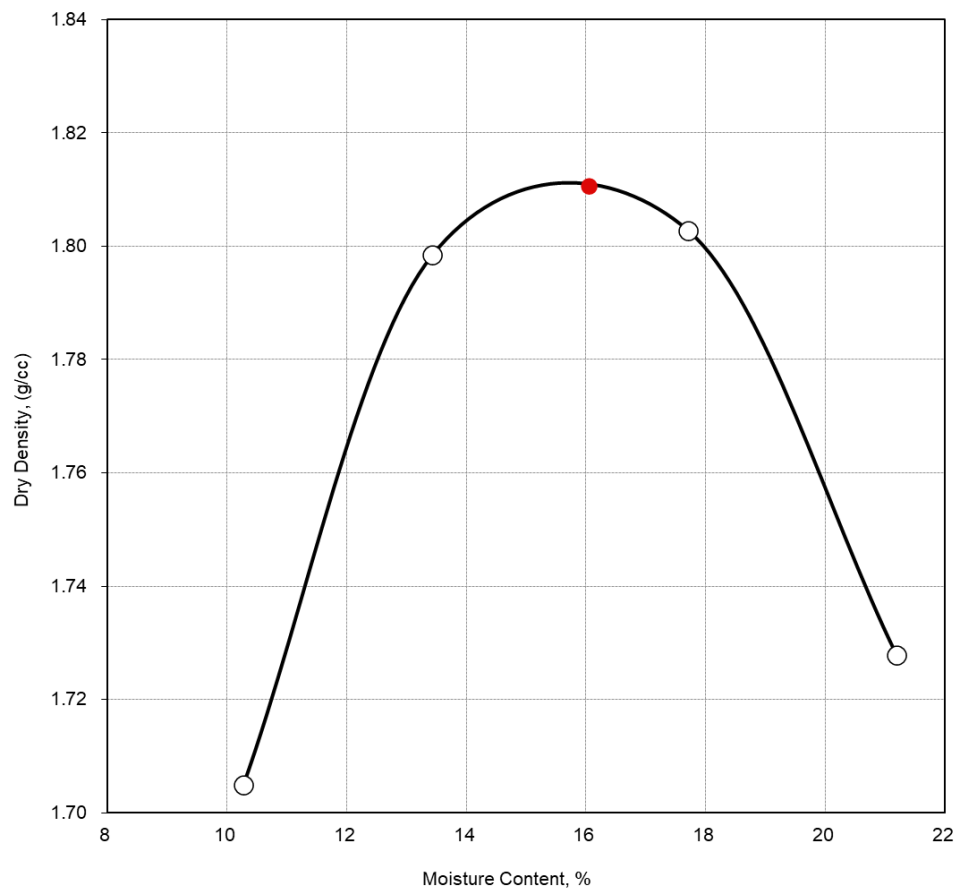


Figure 3.1 Proctor Compaction Curve for Subsoil Sample

Table 3.2 Observation Table for Proctor Compaction Test (Granular Fill Sample)

Determination No.	1	2	3	4
Wt. of mould, m1, g	2028	2028	2028	2028
Wt. of mould + Compacted soil, m2, g	4104	4202	4274	4228
Wt. of compacted soil, (m2-m1), g	2076	2174	2246	2200
Wet Density (g/cc) $\gamma_b = \frac{(m_2 - m_1)}{V_m}, g/cc$	2.08	2.17	2.25	2.20
Moisture Content, %	8.1	9.9	13.1	16.7
Dry density (g/cc) $\gamma_d = \frac{100 \gamma_b}{100 + w}, g/cc$	1.92	1.98	1.99	1.89

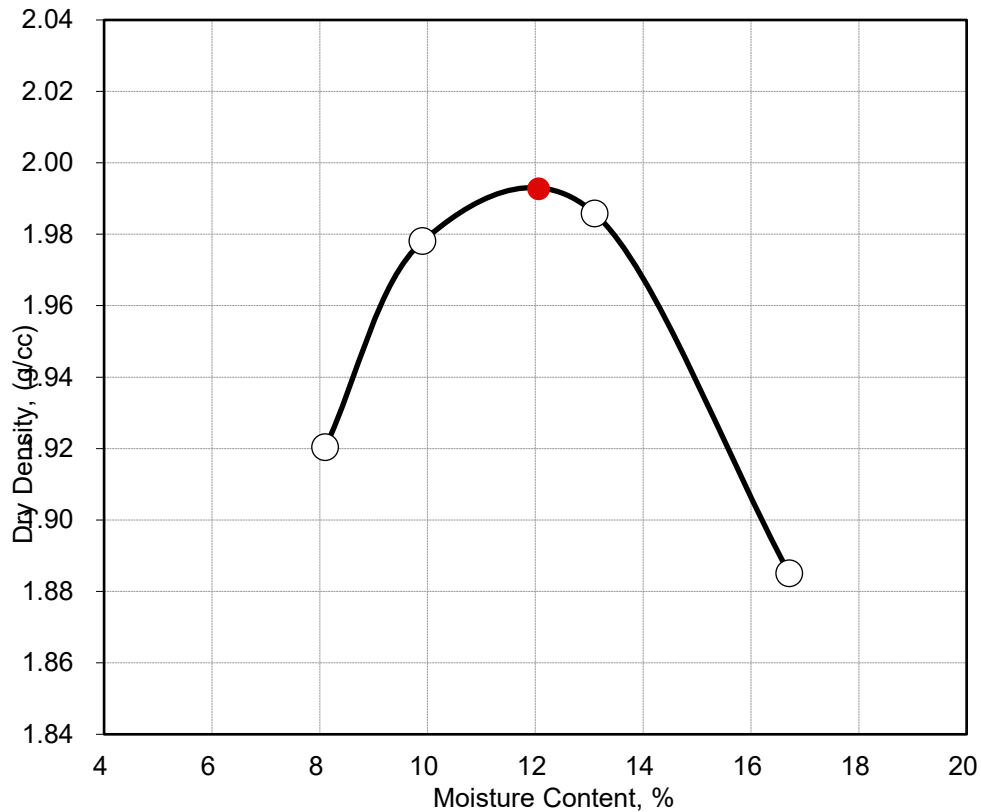


Figure 3.2 Proctor Compaction Curve for Granular Fill Sample

3.2.2 Atterberg Limits Test

The liquid limit (LL) of clayey subsoil was determined in the geotechnical laboratory using the one-point method, which is a simplified approach requiring only a single trial at a specific moisture content. Unlike the conventional multi-point method, this technique significantly reduces the time and effort involved while still providing reasonably accurate results through established correlations.

In this procedure, a soil paste is placed in the Casagrande cup, and a groove is made using a standard tool. The cup is then dropped repeatedly at a controlled rate until the groove closes over a length of 12 mm. The number of blows (N) required for this closure is recorded.

The one-point method is valid only if the number of blows falls within specified ranges:

- 15 to 35 blows for soils with liquid limits below 50%, and
- 20 to 30 blows for soils with liquid limits between 50% and 120%.

Once the number of blows and the corresponding moisture content (W) are determined, the liquid limit at 25 blows is calculated using empirical correlations. This method offers a quick and efficient means of estimating the liquid limit, especially useful for preliminary soil classification and consistency analysis in fine-grained soils.

The plastic limit test was performed in the laboratory to ascertain the water content at which the clayey subsoil transitions from a plastic to a semi-solid state. I sieved the dirt using a 425-micron sieve and subsequently combined it with water to create a malleable mass. Minuscule pieces were shaped into threads on a glass plate until they commenced to disintegrate at a diameter of around 3 mm. The fragmented fragments were gathered for the assessment of moisture content. The determined plastic limit is crucial for soil categorisation and offers insight into the soil's consistency and workability.

Table 3.3 Observation Table for Atterberg Limit Tests (for Subsoil Clayey Sample)

PLASTIC LIMIT	
Wt. Can + Wet. Soil, g	29.005
Wt. Can + Dry. Soil, g	26.312
Wt. Water, g	2.693
Wt. Can, g	18.932
Wt. Dry Soil, g	7.380
Plastic Limit (w_p), %	36.5
LIQUID LIMIT	
No of blows	20
Wt. Can + Wet. Soil, g	52.45
Wt. Can + Dry. Soil, g	35.905
Wt. Water, g	16.545
Wt. Can, g	16.988
Wt. Dry Soil, g	18.917
Water Content, %	87.5

Liquid Limit by one point method is given by:-

$$w_L = \frac{w_n}{1.3215 - 0.23 \log N}$$

Where,

w_L = Liquid Limit

w_n = water content (%) corresponding to “N” blows

$$w_L = 85.6\%$$

$$w_p = 36.5\%$$

$$I_p = w_L - w_p = 49.1\% (> I_p \text{ A-Line, therefore CH})$$

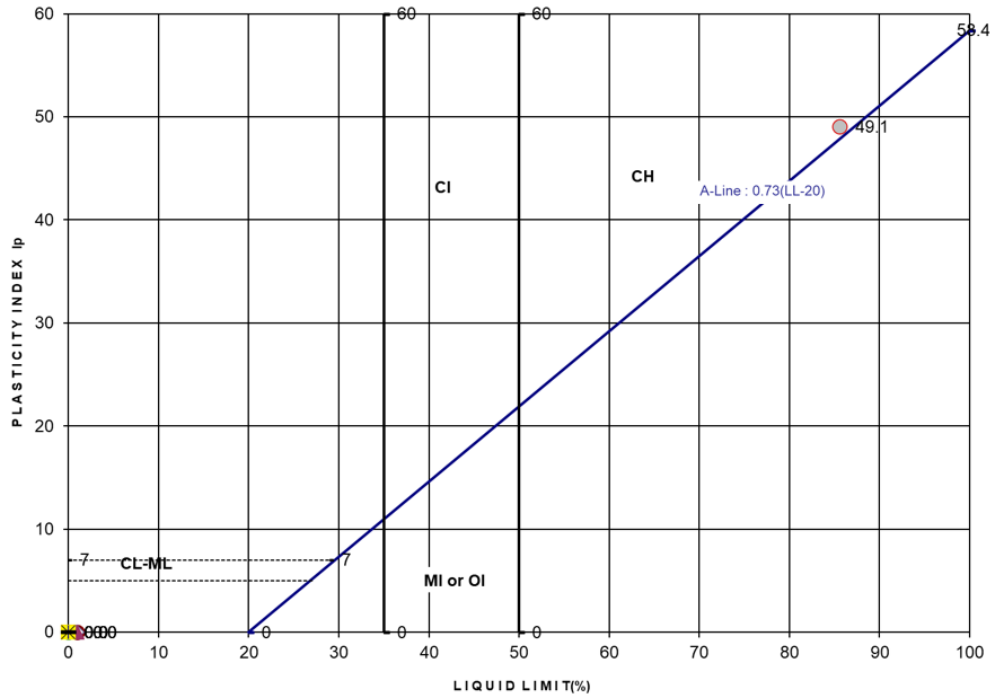


Figure 3.3 Subsoil Clayey Sample represented on plasticity chart

3.2.3 Direct Shear Test

The critical soil parameters related to shear strength, specifically cohesion (c) and the angle of internal friction (ϕ), were determined through laboratory testing using the Direct Shear Test (DST) method. This test was performed in accordance with the procedures outlined in the Indian Standard IS:2720 (Part 13)-1986, which provides the standard guidelines for evaluating the shear strength properties of soil samples.

The shear strength of a soil mass is a fundamental property that defines the maximum shear stress the soil can resist before failure occurs. It plays a vital role in the stability and design of various geotechnical structures, including foundations, embankments, and retaining walls.

In the Direct Shear Test setup, the soil specimen is placed within a shear box that consists of two halves. Flat grid plates are installed at the top and bottom of the soil

sample to provide a uniform surface for load application and to reduce frictional resistance between the soil and the box walls. A loading pad is then placed on the top grid plate, which ensures even distribution of the vertical load applied to the specimen.

To allow relative movement between the two halves of the shear box during the test, a 1 mm clearance gap is maintained between the upper and lower sections of the box. Shear force is gradually applied along the horizontal direction until a total shear displacement of either 12 mm or 20% of the longitudinal length of the sample—whichever occurs first—is reached, signifying the failure point of the sample.

The shear load is transmitted through a proving ring assembly, which precisely measures the applied force. Simultaneously, the corresponding horizontal displacement of the sample is monitored using a horizontal dial gauge for accurate deformation readings.

To ensure reliable and comparative results, the test was conducted three times, each with a different standard vertical load: 0.5 kg/cm², 1.5 kg/cm², and 2.0 kg/cm². For all three tests, a constant strain rate of 1.25 mm/min was maintained throughout the shearing process to ensure uniform loading conditions and to minimize the influence of strain rate variability on the results.

Table 3.4 Observation Table for Direct Shear Test (Granular Fill Sample)

Vertical Pressure kg/cm ²		0.50			1.00			1.50		
Size of Shear Box (cm)		6 X 6			6 X 6			6 X 6		
Rate of Strain mm/min		0.125			0.125			0.125		
Dial Reading	Corrected Area	P.R Dial Reading	Load (kg)	Shear Stress, kg/cm ²	P.R Dial Reading	Load, kg	Shear Stress, kg/cm ²	P.R Dial Reading	Load, kg	Shear Stress, kg/cm ²
0	36.000	0	0.00	0.00	0	0.00	0.00	0	0.00	0.00
10	35.940	7	2.75	0.08	10	3.92	0.11	12	4.71	0.13
20	35.880	11	4.32	0.12	14	5.49	0.15	17	6.67	0.19
30	35.820	14	5.49	0.15	17	6.67	0.19	22	8.63	0.24
50	35.700	17	6.67	0.19	21	8.24	0.23	34	13.33	0.37
100	35.400	20	7.84	0.22	29	11.37	0.32	45	17.64	0.50

200	34.800	24	9.41	0.27	39	15.29	0.44	60	23.51	0.68
300	34.200	26	10.20	0.30	44	17.25	0.50	65	25.47	0.74
400	33.600	28	10.98	0.33	48	18.81	0.56	71	27.81	0.83
500	33.000	25	9.80	0.30	52	20.38	0.62	73	28.59	0.87
600	32.400				50	19.60	0.60	75	29.38	0.91
700	31.800							72	28.20	0.89
Shear Stress at Failure		0.33 kg/cm ²			0.62 kg/cm ²			0.91 kg/cm ²		
Shear Strain at Failure		6.67%			8.83%			10.00%		

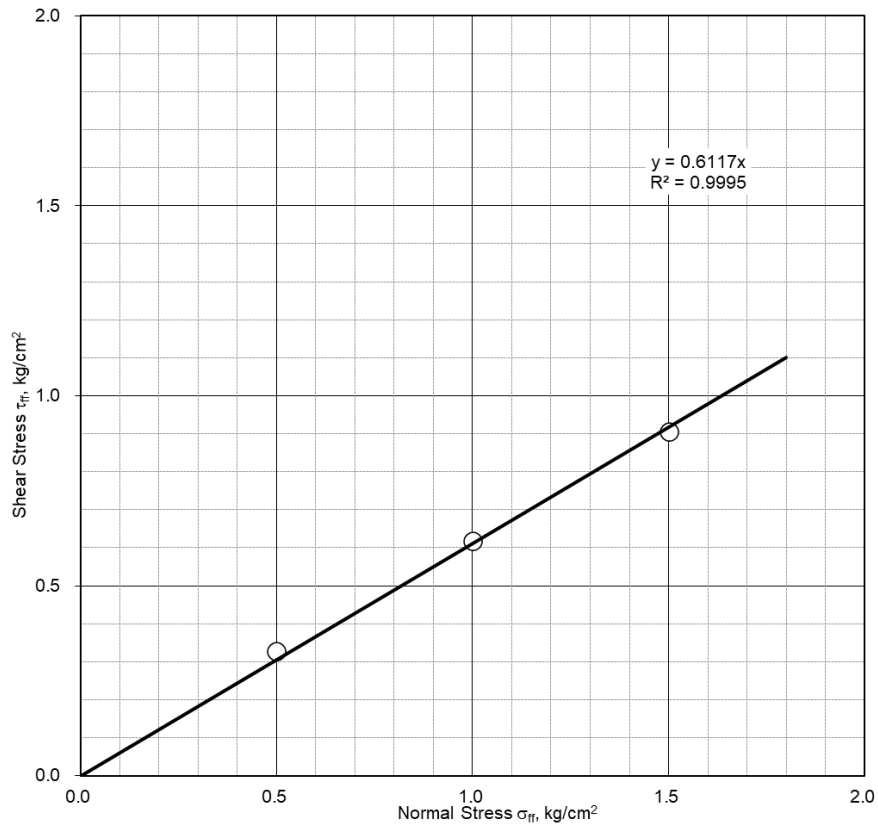


Figure 3.4 Mohr-Coulomb Failure Envelope (for granular fill sample)

Table 3.5 c and Φ values for granular fill sample

c =	0.00 kg/cm ²
tan Φ =	0.612
Φ =	31.5 degrees

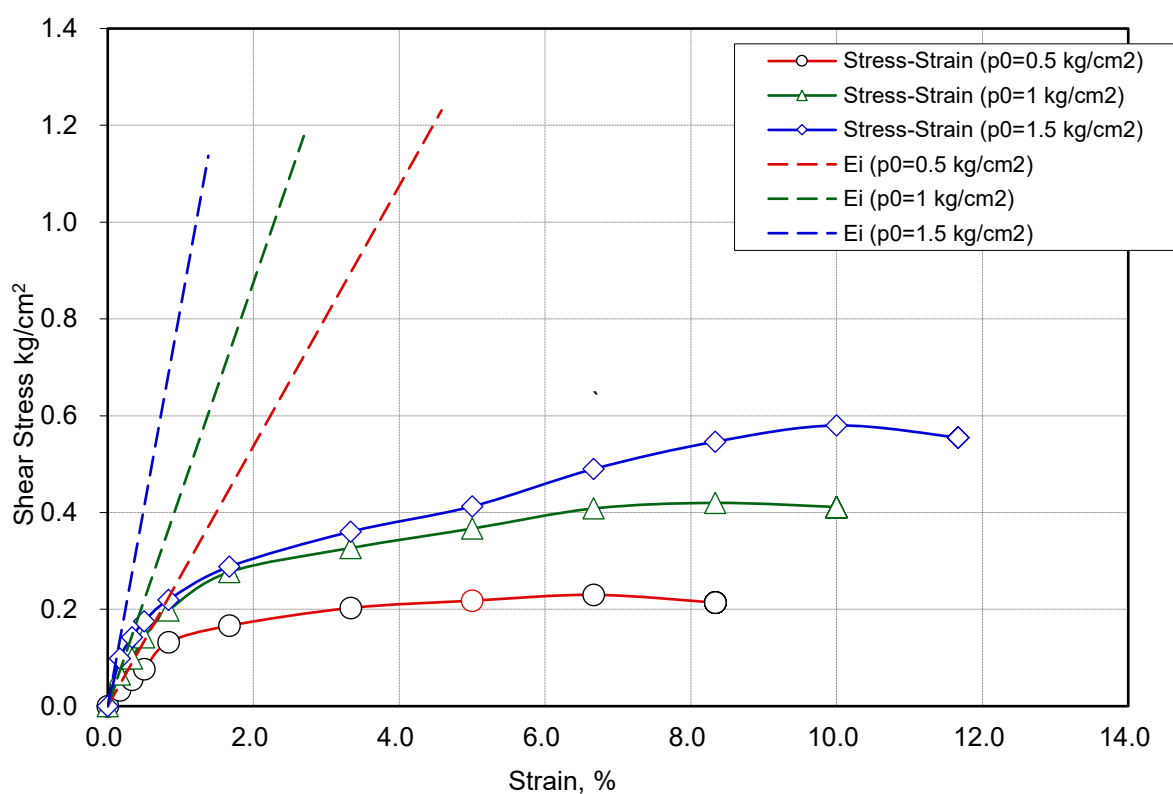


Figure 3.5 Stress-Strain Curve for Granular Fill Sample

Table 3.6 Direct Shear Test Results for Granular Fill Sample

Vertical Pressure, kg/cm ² :	0.5	1.0	1.5
Shear stress at Failure:	0.33	0.66	0.95
Failure Strain, e_f (%):	6.7	8.3	10.0
Initial Tangent Modulus, E_i (kg/cm ²):	27	44	82
Secant Modulus, E_{50} (kg/cm ²):	20	25	51

Table 3.7 Observation Table for Direct Shear Test (Subsoil Sample)

Vertical Pressure kg/cm ²		0.50			1.00			1.50		
Size of Shear Box (cm)		6 X 6			6 X 6			6 X 6		
Rate of Strain mm/min		0.125			0.125			0.125		
Dial Reading	Corrected Area	P.R Dial Reading	Load (kg)	Shear Stress, kg/cm ²	P.R Dial Reading	Load, kg	Shear Stress, kg/cm ²	P.R Dial Reading	Load, kg	Shear Stress, kg/cm ²

0	36.000	0	0.00	0.00	0	0.00	0.00	0	0.00	0.00
10	35.940	3	1.18	0.03	6	2.35	0.07	9	3.53	0.10
20	35.880	5	1.96	0.05	9	3.53	0.10	13	5.10	0.14
30	35.820	7	2.75	0.08	13	5.10	0.14	16	6.28	0.18
50	35.700	12	4.71	0.13	18	7.06	0.20	20	7.84	0.22
100	35.400	15	5.88	0.17	25	9.80	0.28	26	10.20	0.29
200	34.800	18	7.06	0.20	29	11.37	0.33	32	12.55	0.36
300	34.200	19	7.45	0.22	32	12.55	0.37	36	14.12	0.41
400	33.600	20	7.84	0.23	35	13.72	0.41	42	16.47	0.49
500	33.000	18	7.06	0.21	37	14.51	0.42	46	18.03	0.55
600	32.400				34	13.33	0.41	48	18.81	0.58
700	31.800							45	17.64	0.55
Shear Stress at Failure		0.23 kg/cm ²			0.42 kg/cm ²			0.58 kg/cm ²		
Shear Strain at Failure		6.67%			8.83%			10.00%		

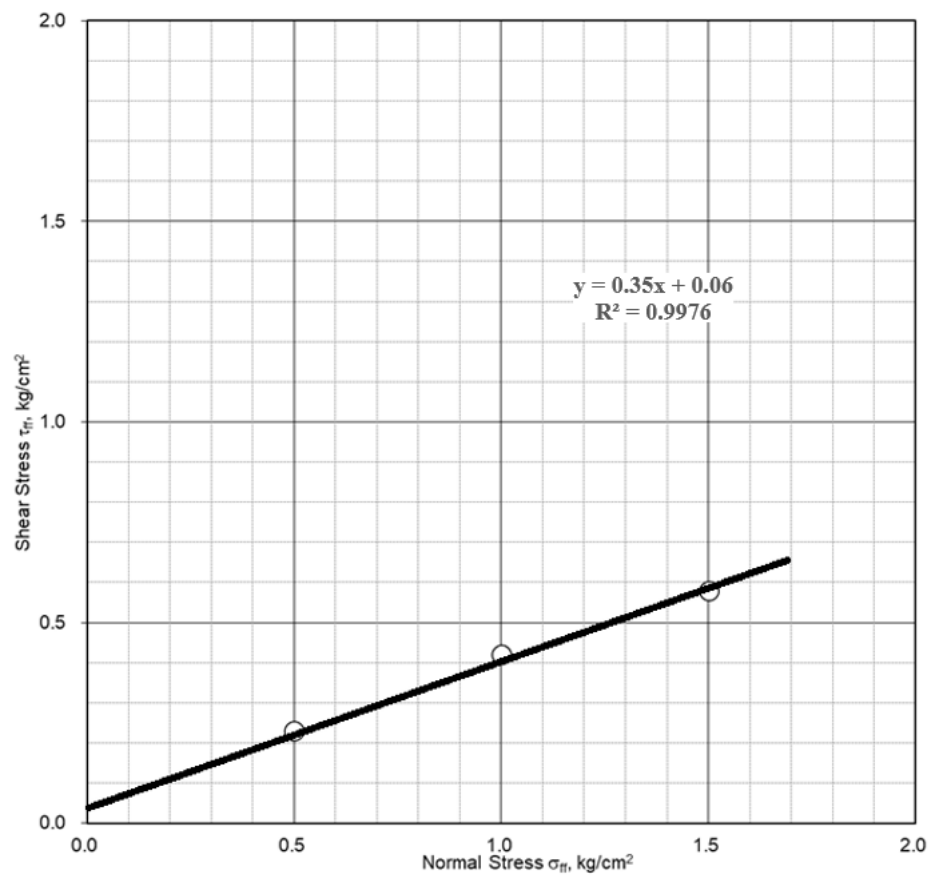
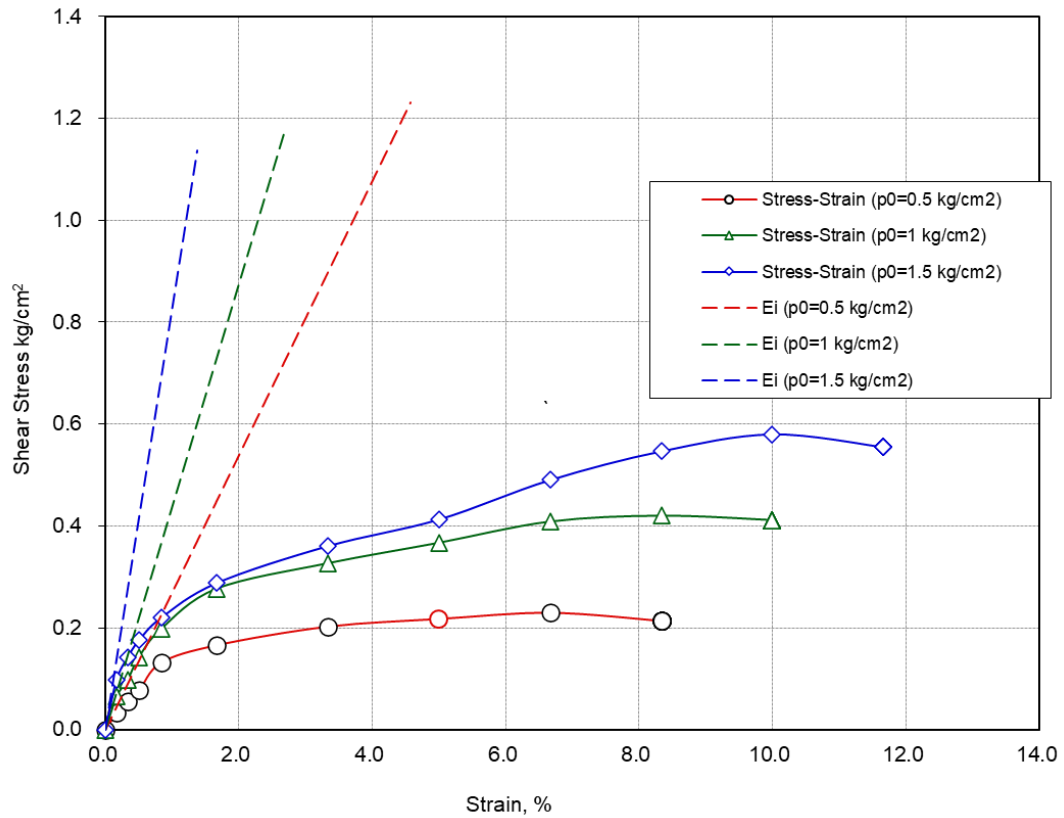


Figure 3.6 Mohr-Coulomb Failure Envelope (for subsoil sample)

Table 3.8 c and Φ values for subsoil sample

$c =$	0.06 kg/cm ²
$\tan \Phi =$	0.35
$\Phi =$	19.2 degrees

**Figure 3.7** Stress-Strain Curve for Subsoil Sample**Table 3.9** Direct Shear Test Results for Subsoil Sample

Vertical Pressure, kg/cm ² :	0.5	1.0	1.5
Shear stress at Failure:	0.23	0.42	0.58
Failure Strain, e_f (%):	6.7	8.3	10.0
Initial Tangent Modulus, E_i (kg/cm ²):	27	44	82
Secant Modulus, E_{50} (kg/cm ²):	16	22	17

3.3 MATREIAL PARAMETES

Table 3.10 Parameters of subsoil and granular fill material samples

Property	Units	Subsoil (soft soil)	Pile Material (Concrete)	Embankment (granular fill)
Unit Weight γ	kN/m ³	17.75	25	19.52
c of soil	kN/m ²	5.88	NA	0
Φ of soil	Degrees	19.2	NA	31.5
Modulus of Elasticity	kN/m ²	5000	25*E6	80000
Poisson's Ratio	NA	0.15	0.2	0.2

Table 3.11 Parameters of geogrid material used (Reference: Appendix-1)

Properties	Units	MD Values	XMD Values
Aperture Dimensions	Mm	38	38
Tensile Strength at 2% Strain	kN/m	8.9	8.9
Minimum rib thickness	Mm	1.1	0.8
Tensile Strength at 5% Strain	kN/m	16.9	16.9
Ultimate Tensile Strength	kN/m	25.0	25.0

Note: In machine direction (MD)

Direction perpendicular to the machine direction (XMD)

3.4 NUMERIACAL MODEELING

A numerical model was developed utilising PLAXIS 2D to examine the performance of a basal reinforced piled embankment system. The model replicated a cross-section of the embankment situated on soft clay, reinforced by piles and a geogrid layer positioned at the foundation. Suitable material characteristics were designated for the embankment fill, soft soil, piling components, and geogrid. Boundary conditions, building phases, and loading parameters were meticulously delineated to simulate field circumstances. The investigation concentrated on assessing settlement reduction, soil

arching, and load transmission mechanisms, yielding significant insights into the performance and efficacy of geosynthetic reinforcement in piled embankment systems.

3.4.1 PLAXIS 2D MODEL

The PLAXIS 2D model depicts a 6-meter-high embankment built on a 12-meter-deep layer of soft clay subsoil. Two unique soil types were identified: soft clay for the subsoil and granular fill for the embankment structure. The pliable clay exhibited poor stiffness and significant compressibility, whereas the granular fill was designated with superior strength and stiffness characteristics. A biaxial geogrid (SQ2525) was utilised at the embankment's base as basal reinforcement to improve stability and mitigate settlement. The model incorporated suitable boundary constraints and sequential building to replicate field circumstances, with the objective of examining load transfer and soil arching behaviour.

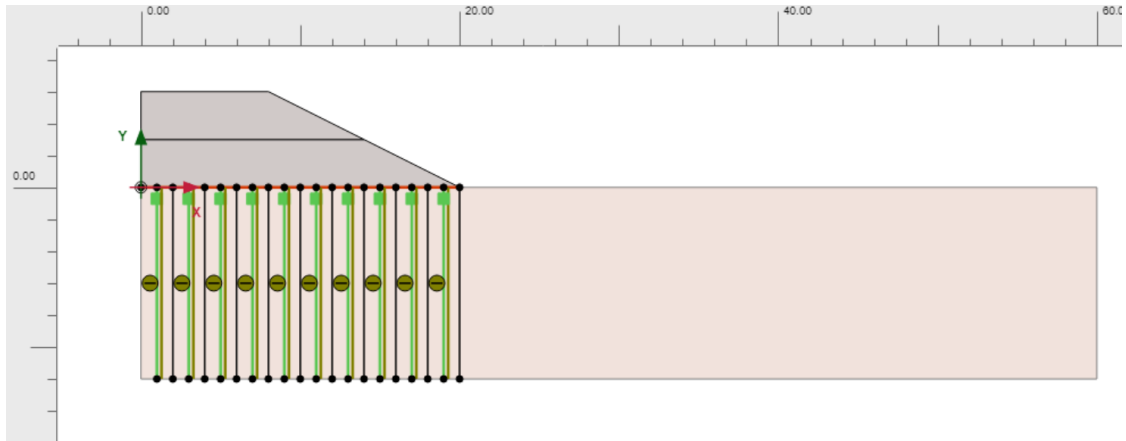


Figure 3.8 Plaxis-2D Model of Basal Reinforced Piled Embankment System

3.4.2 MODEL DETAILS

A numerical investigation was carried out to evaluate the stability of a 6-meter-high embankment constructed over a soft clay foundation. The embankment was analysed using advanced finite element modelling techniques in PLAXIS 2D, which allows for detailed simulation of soil-structure interactions under various loading and boundary conditions. To enhance the stability and reduce settlement of the embankment

constructed on weak subsoil, a combination of pile foundation and geogrid basal reinforcement was adopted as the ground improvement technique.

The soil profile underlying the embankment consists of a 12-meter-deep layer of soft clay, which is generally characterized by low shear strength, high compressibility, and low bearing capacity. This soft clay layer is underlain by a relatively stiffer soil stratum, providing a competent bearing layer for the pile foundation system.

The analytical procedure involved several key steps. Initially, the input parameters related to the embankment fill material, geogrid reinforcement, and subsoil properties were entered into the PLAXIS 2D software. These parameters were determined based on standard geotechnical laboratory tests and relevant material specifications to ensure accurate modelling.

Following this, a detailed numerical model of a basal-reinforced piled embankment was developed. In the analysis, three different pile arrangement patterns were investigated: square, triangular, and rectangular. The piles were modelled with a consistent diameter of 0.30 meters across all configurations. For the rectangular layout, a length-to-breadth (L/B) ratio of 1.2 was considered to compare its performance with the traditional square ($L/B = 1$) and triangular configurations.

The study placed particular emphasis on the impact of pile spacing and arrangement patterns on the load transfer mechanism, settlement behaviour, and overall stability of the embankment. The chosen L/B ratio of 1.2 in the rectangular layout was used to explore whether a non-uniform pile grid offers any structural or economic advantages over conventional symmetrical layouts. The results from this modelling effort provide useful insights into the design optimization of pile-supported embankments reinforced with geogrids for soft ground conditions.

CHAPTER 4

RESULTS AND DISCUSSIONS

4.1 INFLUENCE OF GEOGRID TENSILE STRENGTH AND ANCHORAGE LENGTH ON SAR

The figure 4.1 presented provides a visual representation of the influence of geogrid tensile strength and anchorage length on the Soil Arching Ratio (SAR), a critical parameter in the design and performance assessment of basal reinforced embankments. Specifically, the figure highlights how variations in the tensile strength of the geogrid reinforcement, along with corresponding changes in the anchorage length, affect the development and efficiency of soil arching within the reinforced soil mass.

From the graphical data, it is observed that the Soil Arching Ratio tends to decrease as the tensile strength of the geogrid increases. This trend is further accentuated when there is a simultaneous increase in the anchorage length of the reinforcement. In practical terms, this means that stronger geogrid materials, when anchored over longer lengths, lead to reduced stress transfer from the embankment to the underlying subsoil. This occurs because a more robust reinforcement layer, securely anchored, can more effectively distribute and carry the loads, thereby reducing the stress concentration below.

As indicated in the figure 4.1, a specific SAR value of approximately 0.2 can be achieved when the geogrid possesses a tensile strength of 1,200 kN/m and is anchored with a length of 4.5 meters. This illustrates a balance point where the reinforcement properties are optimized to control subsurface stress effectively.

The Soil Arching Ratio itself is defined as the ratio between the vertical stress experienced by the subsoil and the total vertical stress exerted by the embankment structure. This ratio is largely governed by the membrane effect of the geosynthetic reinforcement, which is directly influenced by the material's tensile strength.

Moreover, extending the length of the basal reinforcement beyond its minimum design requirement contributes to a phenomenon known as self-anchorage. In this condition, the reinforcement system develops internal resistance due to stretching, as

opposed to relying on frictional resistance or slipping. This transition from a slipping mechanism to a stretching mechanism reduces the efficiency of the soil arching effect, and hence, results in a lower Soil Arching Ratio.

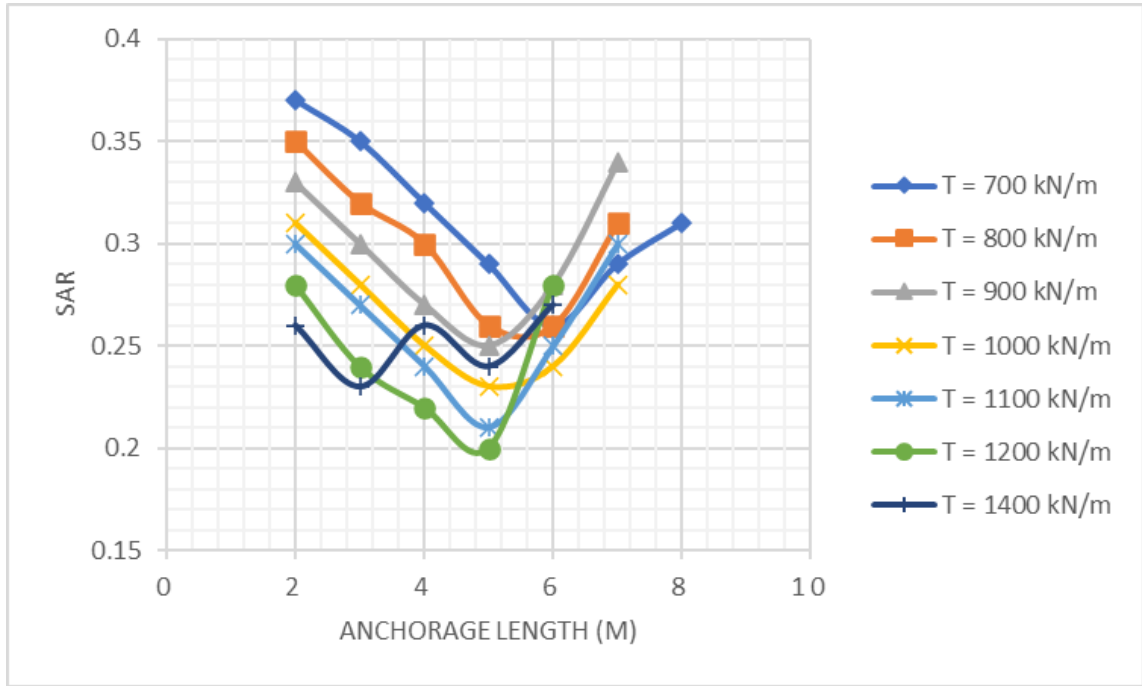


Figure 4.1 Variation of SAR with geogrid anchorage length

4.2 INFLUENCE OF PILE SPACING AND GEOGRID TENSILE STRENGTH ON SAR

The figure provided illustrates the combined influence of pile spacing and the tensile strength of basal reinforcement on the Soil Arching Ratio (SAR), a key indicator of load transfer efficiency in reinforced embankment systems. This graphical representation demonstrates the sensitivity of SAR to changes in the spacing between piles, particularly when the tensile strength of the basal reinforcement is held constant.

According to the data shown in the figure, as the spacing between piles increases, the SAR correspondingly decreases for a given tensile strength of the geosynthetic reinforcement layer. This implies that wider pile spacing reduces the efficiency of load transfer from the embankment to the pile heads, thereby lowering the proportion of stress transmitted through the soil arching mechanism.

Specifically, it is observed that a target SAR value of approximately 0.20 can be successfully attained when the pile spacing is set to 5D (where D is the diameter of the pile) and the basal reinforcement used has a tensile strength of 1200 kN/m. This configuration represents an optimal balance between reinforcement strength and structural layout, allowing for effective interaction between the geogrid and the underlying pile system.

The effectiveness of basal reinforcement in this context is largely due to its ability to develop a membrane effect — a tensioned arching action between the pile caps that redistributes loads away from the weaker subsoil. When the piles are spaced appropriately at around 5D, the reinforcement spanning over them can fully mobilize this membrane effect. This optimal spacing enables the geogrid to stretch and carry loads across the gaps between the piles, enhancing load transfer to the stiffer pile foundations and reducing stress on the soft subsoil.

In summary, the figure underscores the importance of careful consideration of both pile spacing and geogrid tensile strength in achieving a desirable Soil Arching Ratio. Properly designed spacing ensures that the basal reinforcement functions efficiently, maximizing the benefits of the membrane effect and contributing to the overall stability of the embankment system.

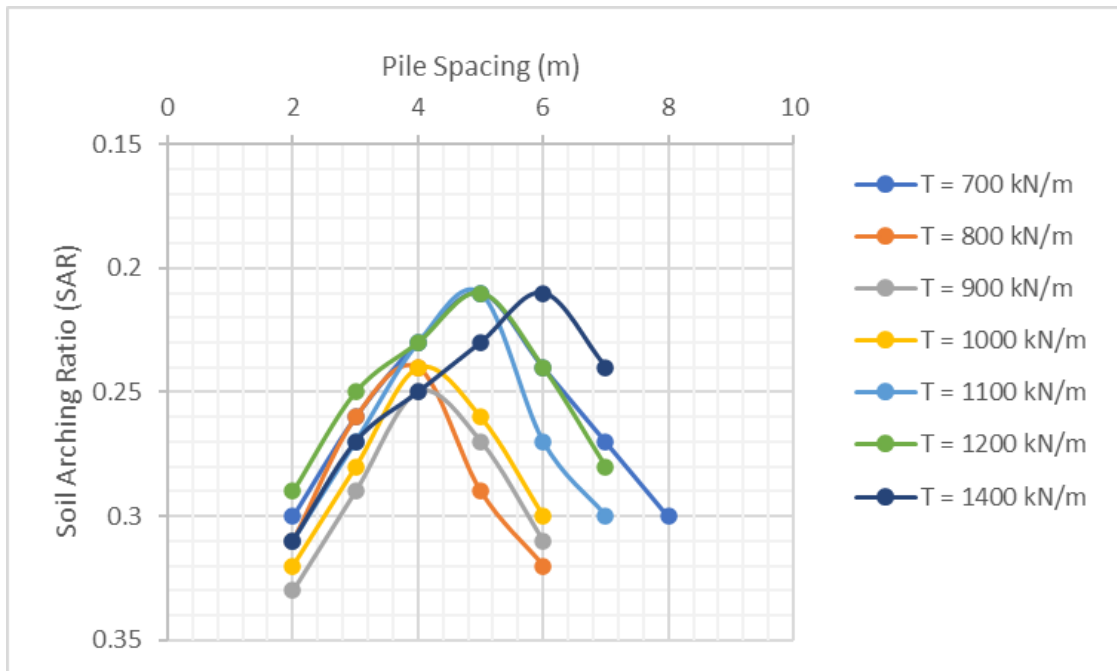


Figure 4.2 Variation of SAR with Pile Spacing

4.3 INFLUENCE OF PATTERN OF PILES ON SAR

In the present study, the configuration of piles was specifically designed in a rectangular arrangement, as opposed to the more conventional square or triangular layouts commonly employed in geotechnical applications. The objective was to assess how the geometry of pile distribution influences the soil arching ratio (SAR), which is a critical factor in load transfer and soil-structure interaction.

The comparative effectiveness of these different pile arrangements is visually represented in the accompanying figure. As illustrated, the rectangular pile configuration—characterized by a length-to-diameter ratio (L/D) of 1.2—consistently outperforms both the square and triangular patterns in terms of enhancing SAR. This suggests that the geometric layout of piles plays a significant role in modifying the load transfer mechanism within the soil.

The improved performance of the rectangular layout can likely be attributed to the transformation of the loading pattern into a more two-dimensional state. Unlike square or triangular configurations, which may concentrate stress in localized zones, the rectangular arrangement promotes a more uniform distribution of stresses. This leads to more efficient mobilization of the surrounding soil, resulting in a higher degree of soil arching and, consequently, better structural support.

In summary, the findings underscore the importance of pile geometry in engineering design and highlight the rectangular configuration as a potentially more effective alternative for optimizing soil-structure interaction, especially in applications where maximizing SAR is a key design objective.

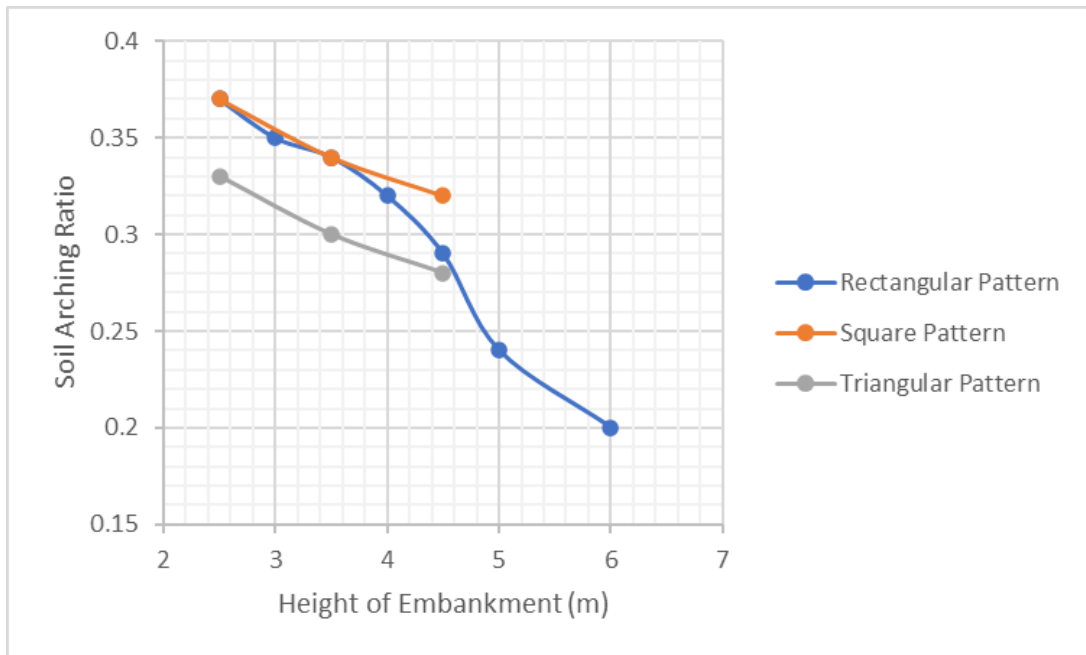


Figure 4.3 Variation of Height of Embankment vs SAR

4.4 INFLUENCE OF NO OF CYCLIC LOADING ON SETTLEMENT

The influence of simulated cyclic loading on both the settlement behaviour of the embankment and the pile head is clearly depicted in the accompanying figure. This analysis was conducted to evaluate the performance and durability of the reinforced embankment system when subjected to repeated loading conditions, which are common in real-world scenarios such as traffic loads, wave action, or seismic activity.

According to the results presented, the embankment reinforced with geosynthetic material experienced a total vertical settlement of approximately 10 millimetres after being subjected to 2000 cycles of cyclic loading. Notably, this settlement trend gradually diminished over time, and the embankment reached a state of stabilization shortly thereafter, indicating no significant further deformation beyond this point.

Similarly, the pile head, which serves as a critical structural component for load transfer, exhibited a much smaller settlement of around 2 millimetres. This settlement occurred relatively quickly—within the first 500 cycles of loading—and subsequently stabilized, showing minimal to no additional movement with continued cyclic loading.

These observed settlement patterns highlight the robust performance of the embankment system, especially when constructed with basal reinforcement over soft clay foundations. The limited and stabilized deformation of both the embankment and the pile head under prolonged cyclic loading conditions underscores the system's ability to maintain structural integrity and load-bearing capacity over time. This suggests that the combined use of piles and geosynthetic reinforcement forms an effective composite structure, capable of mitigating excessive settlement and enhancing the long-term stability of embankments constructed on weak subsoil.

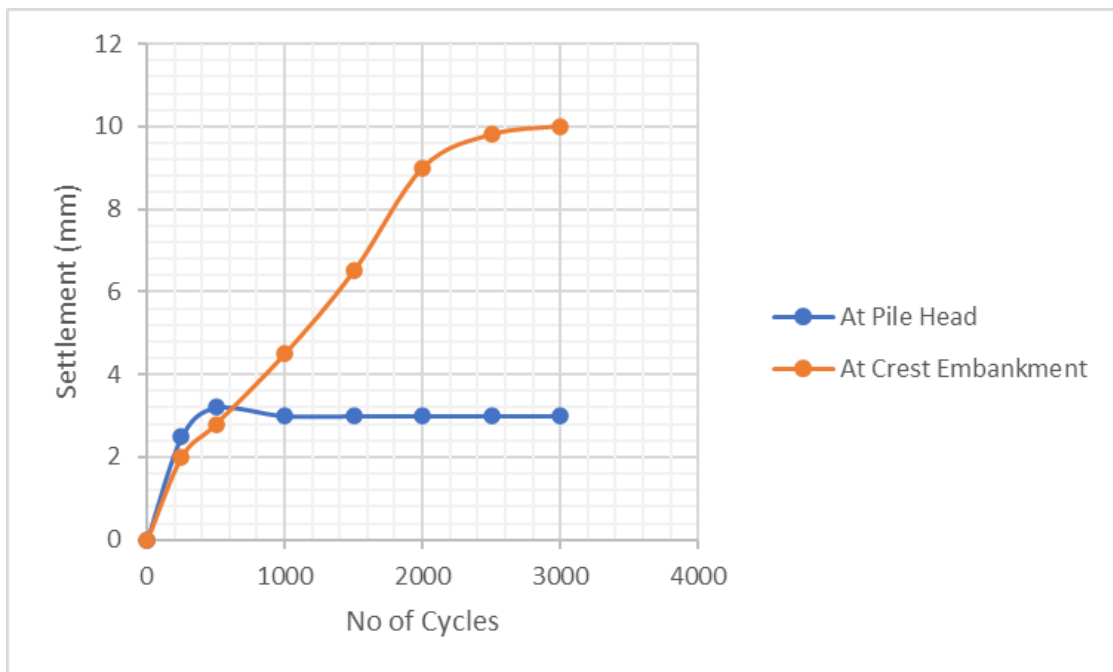


Figure 4.4 Variation of Settlement with number of cycles

4.5 COMPARISON OF RESULTS WITH AND WITHOUT BASAL REINFORCEMENT

4.5.1 Without Basal Reinforcement

The simulation assesses the embankment's performance for excess pore water pressure dissipation and vertical displacements at three representative nodes inside the clay layer.

During embankment building and loading, the soft clay, noted for its low permeability and high compressibility, experiences substantial alterations in pore water pressure resulting from the abrupt increase in vertical stress. Initially, the majority of the applied stress is borne by the pore water, resulting in an elevation of excess pore water pressure. Over time, the surplus pressure steadily diminishes as water exits the soil, leading to an increase in effective stress and consequent settlement.

The graphed excess pore water pressure illustrates a standard consolidation behaviour. Initially, all nodes undergo a significant increase in pore pressure. Over time, pore pressure gradually diminishes, especially in proximity to the pile supports and regions adjacent to drainage pathways. The dissipation rate exhibits minor variations among nodes, contingent upon their depth and closeness to vertical or horizontal drainage limits. The lack of basal reinforcement indicates the absence of supplementary support at the base, which may have facilitated drainage and mitigated lateral spreading.

The displacement graph demonstrates the progressive increase in vertical settlement over time at all monitored nodes. The peak settlement transpires in the soft clay region between the piles, as the embankment load is transmitted via the pliable subsoil. In the absence of basal reinforcement, the load is inadequately distributed laterally, leading to more localised and differential settlements.

The model accurately represents the natural consolidation process in soft clay subjected to embankment stress, characterised by the progressive dissipation of excess pore pressures and a steady increase in settlements. The implementation of pile support facilitates load transmission; nevertheless, without basal reinforcement, the system is susceptible to significant settlements and potential stability concerns, particularly during the first loading stages.

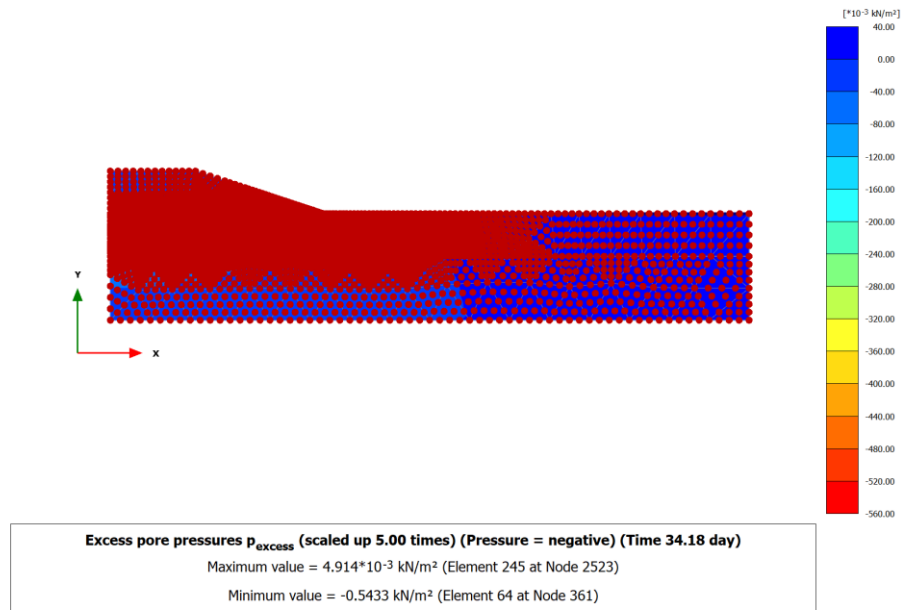


Figure 4.5 Excess Pore Water Pressure dissipation with time

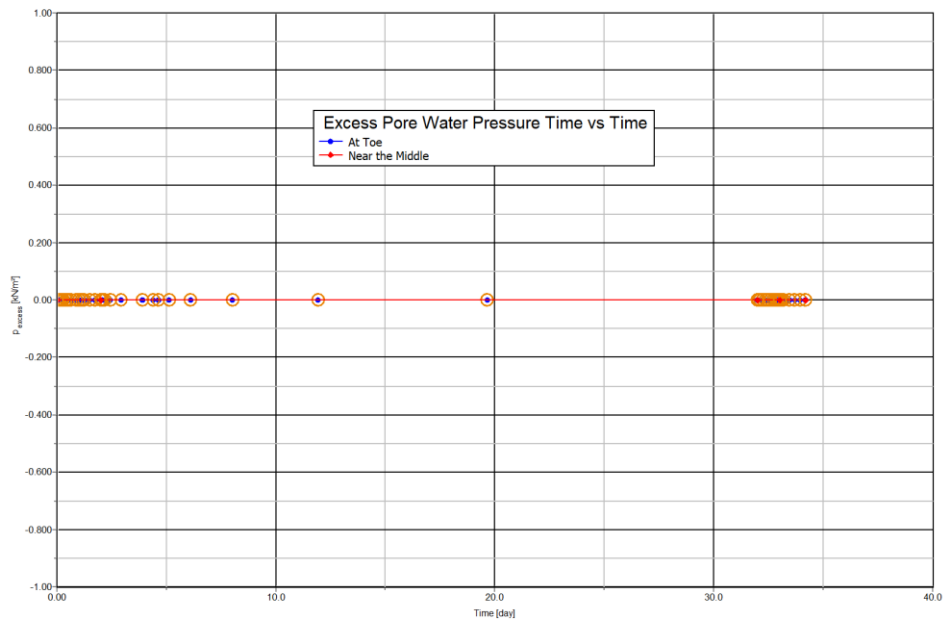


Figure 4.6 Excess Pore Water Pressure vs Time Plot near the middle and at the toe

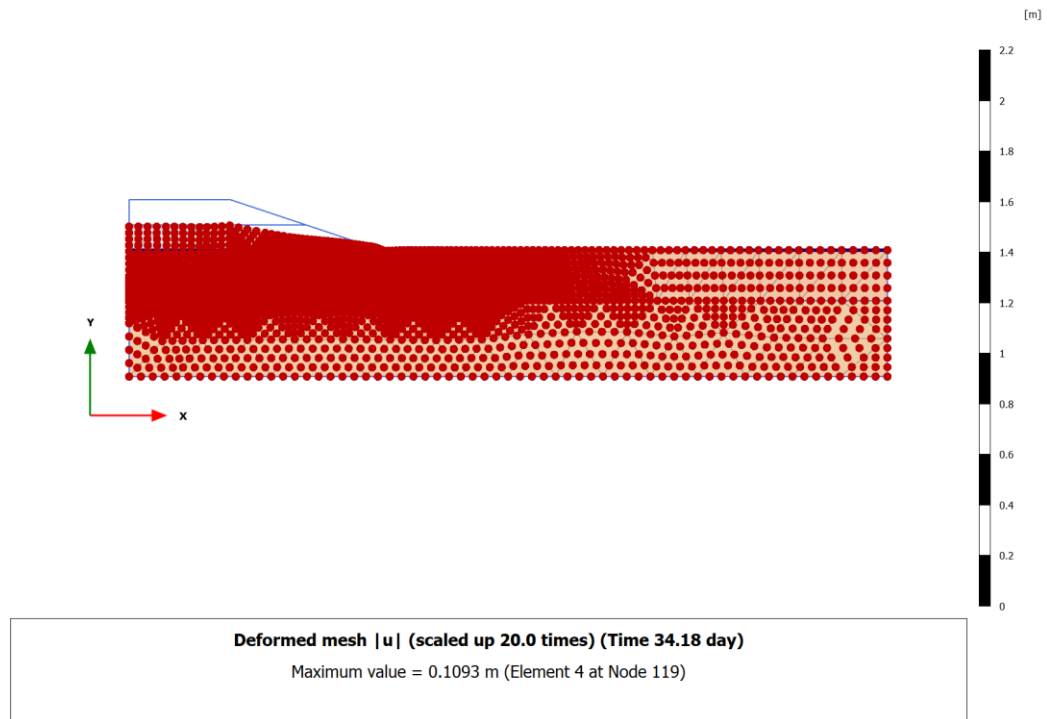


Figure 4.7 Deformation in mesh with time

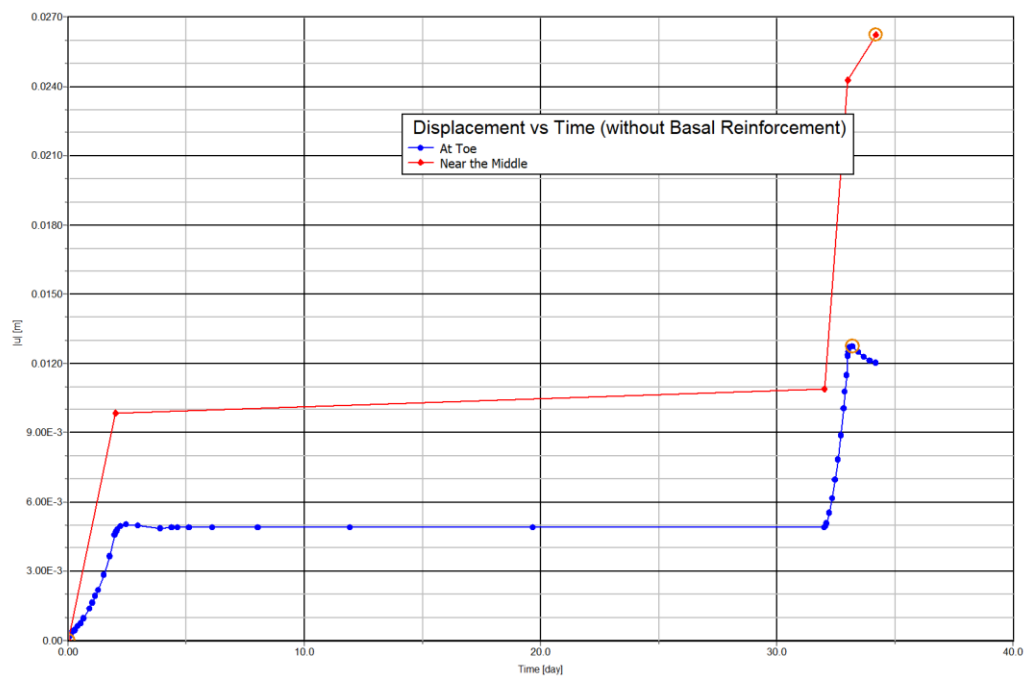


Figure 4.8 Displacement vs Time at the toe and near the middle

4.5.2 With Basal Reinforcement

The incorporation of basal reinforcement, such as geogrid or geotextile layers, substantially affects soil behaviour, especially regarding excess pore water pressure dissipation and vertical displacement (settlement). This form incorporates pile supports, providing a dual mechanism for load transfer and stability.

Upon the construction of the embankment, the soft clay undergoes an instantaneous elevation in vertical tension, resulting in extra pore water pressure attributable to the undrained characteristics of the clay. At first, a significant portion of the applied load is supported by the pore water. Over time, drainage via vertical and lateral routes facilitates water escape, leading to a progressive dissipation of excess pore pressure. The implementation of basal reinforcement facilitates a more uniform distribution of stress over the foundation, hence mitigating localised stress concentrations and expediting consolidation in some regions.

The reinforcement layer functions as a tensioned membrane, offering lateral support at the embankment's base. This improves stability and decreases lateral spreading of the soft clay, which additionally increases drainage by preserving a more stable geometry. Consequently, pore pressure dissipation may transpire more equally, particularly in regions next to the reinforcement.

The use of basal reinforcement mitigates both the extent and variability of vertical displacements in relation to settling. The reinforcement facilitates the connection across soft zones and more efficiently redistributes loads to the pile system. This leads to reduced settlements among the piles and enhanced regulation of overall deformation. The displacement curves at various nodes in the clay will exhibit consolidation-related settlement, but with significantly reduced magnitude relative to an unreinforced scenario.

The incorporation of basal reinforcement in a soft soil embankment model markedly enhances pore pressure dissipation patterns and settling behaviour. It augments pile support by improving load distribution, strengthening stability, and minimising deformation, resulting in a more efficient and secure embankment system.

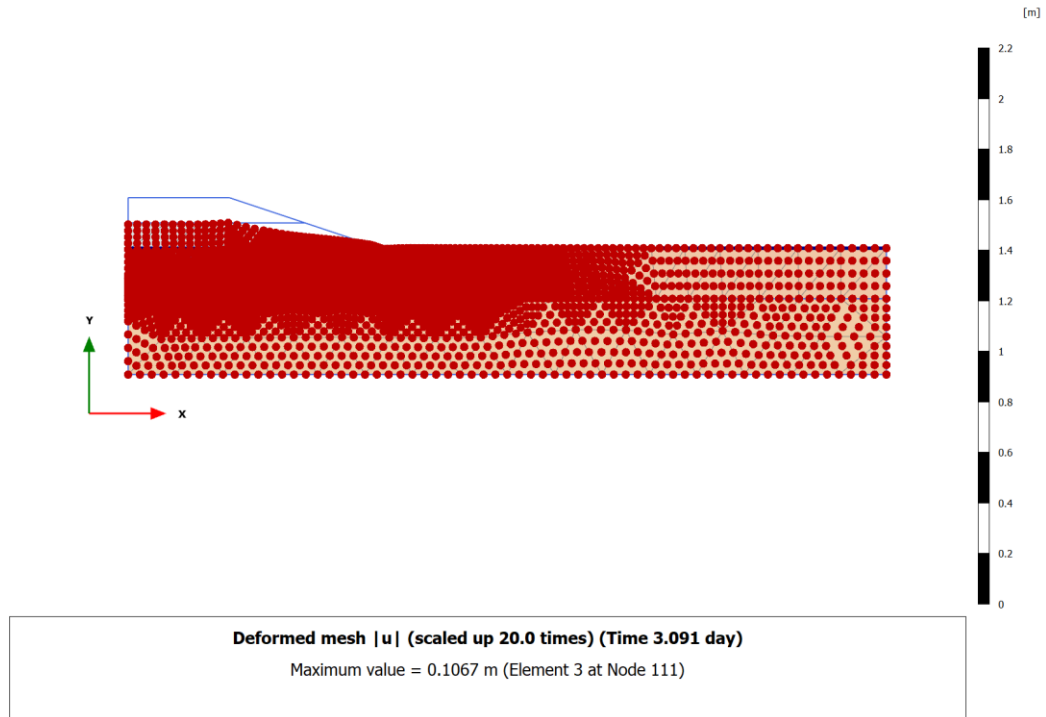


Figure 4.9 Deformed mesh (with Basal Reinforcement)

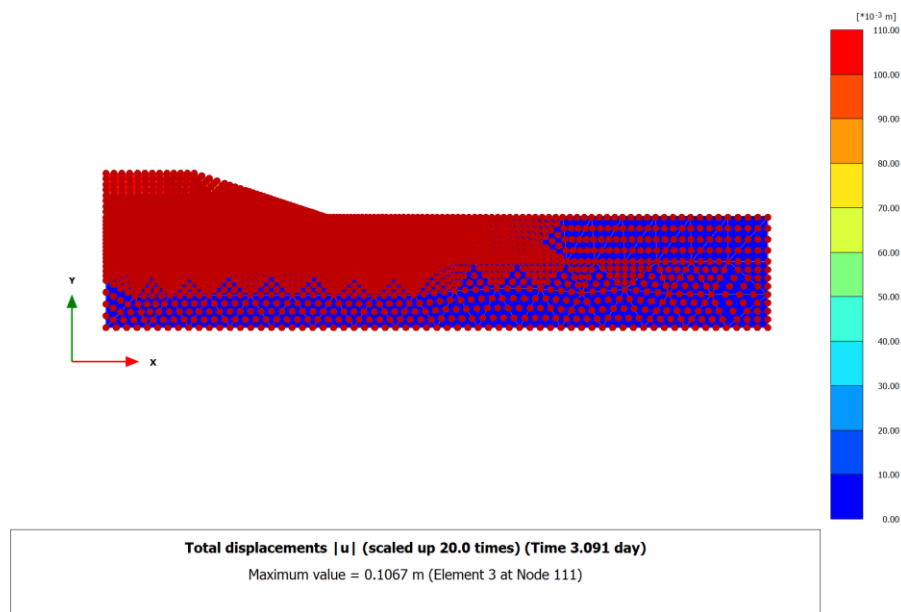


Figure 4.10 Displacements with time (with Basal Reinforcement)

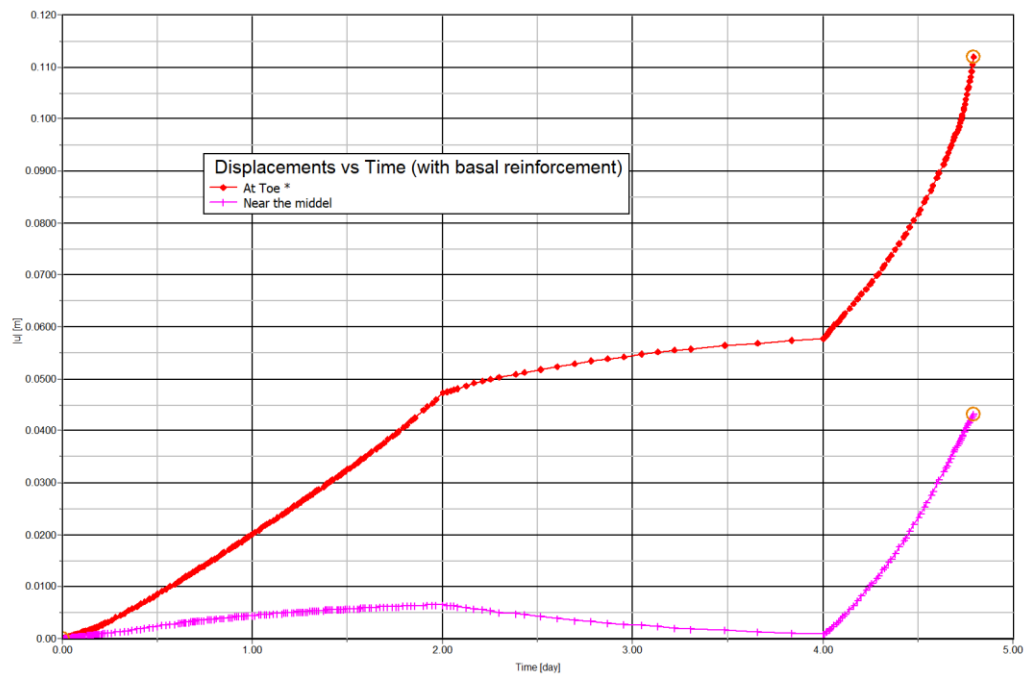


Figure 4.11 Displacements vs Time (with Basal Reinforcement)

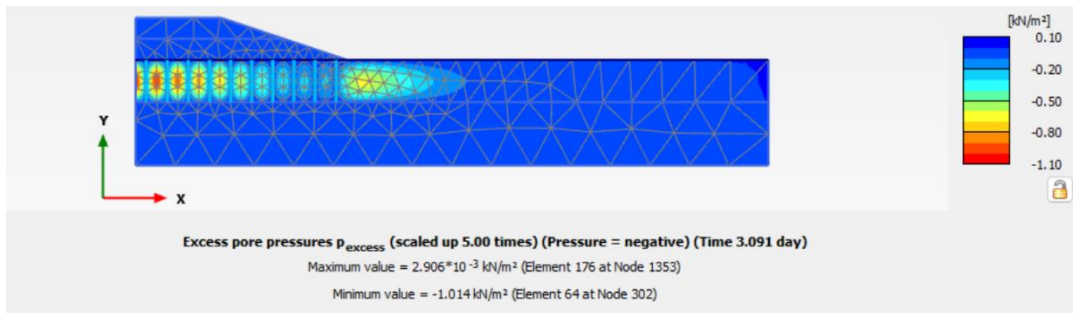


Figure 4. 12 Excess Pore Water Pressure dissipation with basal reinforcement

CHAPTER 5

CONCLUSIONS

The following conclusions have been drawn based on the comprehensive analytical investigation conducted in this study. These insights contribute valuable knowledge to the design and construction of embankments on soft soil using geosynthetic-reinforced pile-supported systems.

5.1 OPTIMAL TENSILE STRENGTH AND PILE SPACING RELATIONSHIP

One of the critical outcomes of this study is the identification of an optimal tensile strength for the geogrid used in basal reinforcement. For a given soft ground condition, the efficiency and cost-effectiveness of embankment construction can be significantly influenced by choosing an appropriate tensile strength for the geogrid. In the simulated model conditions adopted in this study, a tensile strength of **1200 kN/m** was found to be optimal. This tensile strength level allows for an ideal pile spacing of $5D$, where D is the pile diameter, corresponding to a desired Soil Arching Ratio (SAR) of **0.20**.

Increasing the tensile strength beyond 1200 kN/m does not provide any further benefits in terms of SAR enhancement. This indicates that there is a threshold beyond which the tensile contribution of the geogrid is no longer the limiting factor in the system's load transfer behaviour. Hence, using geogrids with higher tensile strengths may result in unnecessary expenditure without corresponding structural benefits.

5.2 ANCHORAGE LENGTH REQUIREMENT

The ability of a geogrid to effectively develop tensile force depends significantly on its anchorage length. Anchorage length is defined as the embedded length of the geogrid required for it to fully mobilize its tensile strength. The results from the numerical modeling reveal that an anchorage length of approximately **4.5 meters** is necessary to activate the tensile capacity of the geogrid under the specified loading and soil conditions. If the anchorage length is insufficient, the geogrid may not fully

contribute to load transfer, compromising the efficiency of the soil arching mechanism. This highlights the need for careful consideration of geogrid embedment during design.

5.3 PERFORMANCE UNDER CYCLIC LOADING AND SETTLEMENT BEHAVIOUR

The basal reinforced pile-supported system exhibits excellent performance under repeated loading. This is especially important for embankments, which may be subjected to dynamic or cyclic loading due to traffic or environmental conditions. In the study, the system demonstrated a **settlement of only 2 mm at the pile head**, even after exposure to **2000 cycles** of simulated loading. Beyond this point, the settlement remained relatively constant, indicating that the system had stabilized. Such a low and stable settlement response is a strong indicator of the structural integrity and long-term serviceability of the embankment.

Moreover, the **total settlement at the crest of the embankment**, though slightly higher due to soil compression and load distribution across the geogrid, remained within acceptable limits. The minimal differential settlement between the pile head and the crest indicates effective load transfer through the geogrid and sufficient confinement of the fill material. It is also noteworthy that the pile tips are founded on a rigid stratum, which further limits downward movement and helps achieve a stable foundation condition.

5.4 PILE ARRANGMENT GEOMETRY AND LOAD DISTRIBUTION

Another important conclusion from this study relates to the geometry of the pile arrangement. Traditional configurations such as **square and triangular** pile layouts have been widely used in practice. However, the results of this investigation suggest that a **rectangular arrangement** of piles, particularly with a **length-to-breadth (L/B) ratio of 1.2**, offers better performance.

This improved behaviour is attributed to the change in load distribution patterns under the embankment. The rectangular layout alters the interaction between soil and reinforcement from a symmetrical (square or triangular) pattern to a more directional, two-dimensional load transfer mechanism. This change enhances the efficiency of the

soil arching process and allows for a more uniform distribution of loads to the piles. As a result, stress concentrations are reduced, and differential settlements are minimized.

5.5 COST EFFICIENCY THROUGH REINFORCEMENT THROUGH REINFORCEMENT OPTIMISATION

A major practical implication of this research is its contribution to cost-effective embankment design. The study strongly supports the notion that **enhancing the tensile strength of the geosynthetic reinforcement** can be a more viable and economical solution than **reducing pile spacing**—a method that significantly increases construction costs due to more frequent pile installations.

By selecting the right tensile strength for the geogrid and optimizing its layout and anchorage, engineers can reduce reliance on dense piling patterns without sacrificing structural performance. This approach is particularly beneficial for supporting area loads, such as those experienced in embankments and roadways, where load distribution is relatively uniform. With proper design, geosynthetic-reinforced pile-supported embankments can achieve the necessary stability and serviceability at a significantly reduced cost.

5.6 FINAL REMARKS

The findings of this study provide valuable guidelines for geotechnical and structural engineers involved in the design of embankments over soft clay soils. By optimizing reinforcement properties and pile layout, substantial improvements in load transfer, settlement control, and cost-efficiency can be realized. Future studies could further explore the long-term behaviour of such systems under varying environmental conditions and loading scenarios to validate and enhance the current recommendations.

APPENDIX-1

Product Data Sheet- Biaxial Geogrid SQ 2525



Tensor, A Division of CMC
2500 Northwinds Parkway, Suite 500
Alpharetta, Georgia 30009 800-TENSAR-1
www.tensorcorp.com

Product Data Sheet – Biaxial Geogrid SQ2525

Product Type:	Integrally Formed Biaxial Geogrid
Polymer:	Polypropylene
Load Transfer Mechanism:	Positive Mechanical Interlock
Primary Applications:	Subgrade Improvement and Base Stabilization

This product has been tested for quality control purposes in a GAI-LAP accredited laboratory, it is part of the AASHTO SSGEO Product Evaluation and Audit Solutions program (formerly known as NTPEP), and it is made in the USA.

Product Properties

Index Properties	Units	MD Values	XMD Values
• Aperture Dimensions ²	mm (in)	38 (1.5)	38 (1.5)
• Rib Thickness ²	mm (in)	1.1 (0.04)	0.8 (0.03)
• Tensile Strength @2% Strain ³	kN/m (lb/ft)	8.9 (610)	8.9 (610)
• Tensile Strength @5% Strain ³	kN/m (lb/ft)	16.9 (1,160)	16.9 (1,160)
• Ultimate Tensile Strength ³	kN/m (lb/ft)	25.0 (1,710)	25.0 (1,710)
Structural Integrity			
• Junction Efficiency ⁴	%		93
• Overall Flexural Rigidity ⁵	mg-cm		1,350,000
• Aperture Stability ⁶	m-N/deg		0.60
Durability			
• Resistance to Long Term Degradation ⁷	%		100
• Resistance to UV Degradation ⁸	%		98

Dimensions and Delivery

The biaxial geogrid shall be delivered to the job site in roll form with each roll individually identified and nominally measuring 12.5 feet (3.8 meters) in width and 164 feet (50 meters) in length.

Notes

1. Unless indicated otherwise, values shown are minimum average roll values determined in accordance with ASTM D4759-02.
2. Nominal dimensions.
3. Determined in accordance with ASTM D6637-10 Method A. This product is intended for soil stabilization purposes only. The long-term creep performance of this product has not been characterized, and therefore, it is not suitable for long-term load support applications.
4. Load transfer capability determined in accordance with ASTM D7737-11.
5. Resistance to bending force determined in accordance with ASTM D7748/D7748M-14.
6. Resistance to in-plane rotational movement measured in accordance with ASTM D7864/D7864M-15.
7. Resistance to loss of load capacity or structural integrity when subjected to chemically aggressive environments in accordance with EPA 9090 immersion testing.
8. Resistance to loss of load capacity or structural integrity when subjected to 500 hours of ultraviolet light and aggressive weathering in accordance with ASTM D4355-05.

Tensor reserves the right to change its Product Data Sheet at any time. It is the responsibility of the person specifying the use of this product and of the purchaser to ensure that Product Data Sheet relied upon for procurement purposes are current and that the product is suitable for its intended use in each instance.

Tensor warrants that at the time of delivery the geogrid furnished hereunder shall conform to the Product Data stated herein. Any other warranty including merchantability and fitness for a particular purpose, are hereby excluded. If the geogrid does not meet the specifications on this page and Tensor is notified prior to installation, Tensor will replace the geogrid at no cost to the customer. This Product Data Sheet (PDS) supersedes all prior PDS for the product described above and is not applicable to any products shipped prior to February 1, 2013 (12/20/2024).



**PRODUCT
EVALUATION
& AUDIT**
SOLUTIONS

References

- [1] I. R. Congress, "Guidelines for the Design and Construction of Geosynthetic Reinforced Embankments on Soft Subsoils," in *IRC-113*, New Delhi, 2013.
- [2] P. J. B. Žlender, "Optimal design of piled embankments with basal reinforcement," *Geosynthetics International*, vol. 25, no. 2, pp. 150-163, 2018.
- [3] M. R. A. & M. S. S. Gonbad, "Enhancement of soil–geogrid interactions in direct shear mode using attached elements as anchors," *European Journal of Environmental and Civil Engineering*, vol. 24, no. 8, pp. 1161-1179, 2020.
- [4] C.-N. Liu, "Behavior of geogrid–reinforced sand and effect of reinforcement anchorage in large-scale plane strain compression," *Geotextiles and Geomembranes*, vol. 42, no. 5, pp. 479-493, 2014.
- [5] S. Abdi-Goudarzi, "An experimental evaluation of geocomposite-reinforced soil sections," *Construction and Building Materials*, vol. 314 Part B , 2022.
- [6] J. Derksen, "Geogrid-soil interaction: experimental analysis of factors influencing load transfer," *Geosynthetics International*, vol. 30, no. 3, pp. 315-336, 2022.
- [7] G. T. Mehrjardi, "Scale effect on the behaviour of geogrid-reinforced soil under repeated loads," *Geotextiles and Geomembranes*, vol. 45, no. 6, pp. 603-615, 2017.
- [8] Y. Jia, "DEM study on shear behavior of geogrid-soil interfaces subjected to shear in different directions," *Computers and Geotechnics*, vol. 156, 2023.
- [9] H. Ahmad, "Effect of the interfacial shearing stress of soil–geogrid interaction on the bearing capacity of geogrid-reinforced sand," *Innovative Infrastructure Solutions*, vol. 6, 2021.
- [10] H. Ahmad, "Scale effect study on the modulus of subgrade reaction of geogrid-reinforced soil," *SN Applied Sciences*, vol. 2, p. article number 394, 2020.
- [11] M. T. & M. M. H. Hasan Ghasemzadeh, "Numerical Analysis of Pile–Soil–Pile Interaction in Pile Groups with Batter Piles," *Geotechnical and Geological Engineering*, vol. 36, p. 2189–2215, 2018.
- [12] V. V. a. M. Muthukumar, "Experimental and numerical study of group effect on the behavior of helical piles in soft clays under uplift and lateral loading," *Ocean Engineering*, vol. 268, 2023.
- [13] Q. Fang, "Influence of Test Method and Poisson' s Ratio Effect on Pullout Performance of Anchor Bolt in Pile," *KSCE Journal of Civil Engineering*, vol. 24, no. 12, pp. 3775-3784, 2020.
- [14] R. Deendayal, "Analysis of laterally loaded group of piles located on sloping ground," *International Journal of Geotechnical Engineering* , vol. 14, no. 5, pp. 580-588, 2020.

- [15] Y. Zhuang, "The load transfer mechanism in reinforced piled embankment under cyclic loading and unloading," *European Journal of Environmental and Civil Engineering*, vol. 26, no. 4, pp. 1364-1378, 2022.
- [16] K. Aqoub, "Quantitative analysis of shallow unreinforced and reinforced piled embankments with different heights subject to cyclic loads: Experimental study," *Soil Dynamics and Earthquake Engineering*, vol. 138, 2020.
- [17] T. A. Pham, "Numerical Analysis of Geosynthetic-Reinforced and Pile-Supported Embankments Considering Integrated Soil-Structure Interactions," *Geotechnical and Geological Engineering*, vol. 42, p. 185–206, 2024.
- [18] C. X. X. Z. P. S. a. M. L. G Li, "Influences of number of geosynthetic reinforcement layers on soil arching under cyclic loading," in *IOP Conference Series: Earth and Environmental Science*, Shanghai, 2024.
- [19] J. Sharma, "Centrifuge modelling of an embankment on soft clay reinforced with a geogrid," *Geotextiles and Geomembranes*, vol. 14, no. 1, pp. 1-17.
- [20] Y. Z. z. a. K. Y. Wang, "Finite-Element Analysis on the Effect of Subsoil in Reinforced Piled Embankments and Comparison with Theoretical Method Predictions," *International Journal of Geomechanics*, vol. 16, no. 5, 2016.
- [21] N. Zhang, "Evaluation of effect of basal geotextile reinforcement under embankment loading on soft marine deposits," *Geotextiles and Geomembranes*, vol. 43, no. 6, pp. 506-514, 2015.
- [22] K. Y. W. & H. L. L. Yan Zhuang, "A simplified model to analyze the reinforced piled embankments," *Geotextiles and Geomembranes*, vol. 42, no. 2, pp. 154-165, 2014.
- [23] R. Rui, "Two-dimensional soil arching evolution in geosynthetic-reinforced pile-supported embankments over voids," *Geotextiles and Geomembranes*, vol. 50, no. 1, pp. 82-98, 2022.
- [24] R. K. R. K.-W. Liu, "Numerical modelling of prefabricated vertical drains and surcharge on reinforced floating column-supported embankment behaviour," *Geotextiles and Geomembranes*, vol. 43, no. 6, pp. 493-505, 2015.
- [25] X.-Y. C. Yan Zhuang, "A simple design approach to analyse the piled embankment including tensile reinforcement and subsoil contributions," *Geotextiles and Geomembranes*, vol. 49, no. 2, pp. 466-474, 2021.
- [26] M. D. J. V. Martina Holíčková, "Testing of Subsoil Support in Physical Model of Piled Embankment," *Transportation Research Procedia*, vol. 40, pp. 711-717, 2019.
- [27] P. L. C. L. K. L. D.T. Bergado, "Performance of reinforced embankment on soft Bangkok clay with high-strength geotextile reinforcement," *Geotextiles and Geomembranes*, vol. 13, no. 6-7, pp. 403-420, 1994.

- [28] T. H. W. D. Jin-chun Chai, "Progressive yielding/softening of soil–cement columns under embankment loading: a case study," *Acta Geotechnica*, vol. 19, p. 7229–7241, 2024.
- [29] R. K. R. a. A. L. Li, "Geosynthetic-reinforced embankments over soft foundations," *Geosynthetics International*, vol. 12, no. 1, pp. 50-85, 2005.
- [30] D. D. O. J. Jiamin Zhang, "3D numerical modeling of a rigid inclusion reinforced railway embankment under cyclic loading," *Transportation Geotechnics*, vol. 41, 2023.
- [31] C. Y. J.-F. C. Z.-A. G. Xu Zhang, "Numerical modeling of floating geosynthetic-encased stone column–supported embankments with basal reinforcement," *Geotextiles and Geomembranes*, vol. 50, no. 4, pp. 720-736, 2022.
- [32] A. S. Z. A. S. Abdul Salam Brohi, "3D Numerical Modeling of Pile embankment performance," *International Journal of Emerging Trends in Engineering Research*, vol. 9, no. 6, 2021.
- [33] M. M. Venkatesan Vignesh, "Experimental and numerical study of group effect on the behavior of helical piles in soft clays under uplift and lateral loading," *Ocean Engineering*, vol. 268, 2023.
- [34] J. L. Per Gunnvard, "Evaluating the Design Criteria for Light Embankment Piling: Timber Piles in Road and Railway Foundations," *Applied Sciences*, vol. 12, no. 1, 2021.
- [35] M. W. Z. Z. Guan-Bao Ye, "Geosynthetic-reinforced pile-supported embankments with caps in a triangular pattern over soft clay," *Geotextiles and Geomembranes*, vol. 48, no. 1, pp. 52-61, 2020.
- [36] S. W. Peng Zhou, "Topology optimization of the periodic pile barrier with initial stresses arranged in rectangular and equilateral triangular lattices," *Structures*, vol. 51, pp. 628-639, 2023.
- [37] W. J. R. B. S. K. S. S. a. P. J. Suttikarn Panomchaivath, "Prediction of Undrained Lateral Capacity of Free-Head Rectangular Pile in Clay Using Finite Element Limit Analysis and Artificial Neural Network," *Engineered Science*, vol. 24, p. 923, 2023.

LIST OF PUBLICATION

S.No	Paper title	Category	Presented in	Publishing in	Status
1	Analytical Study on performance of basal reinforced piled embankment	Conference	Abstract submission for International Conference on Emerging Trends in Engineering (GLS), 20 July, 2025	Yet to be decided	Accepted in conference



SFE
SOCIETY FOR EDUCATION

International Conference on Emerging Trends in Engineering , Science and Technology(ICEST-25)

20th July 2025 | Vadodara - India

Acceptance Letter

Paper ID: SFE_32671

Paper Title: Analytical study on performance of basal reinforced piled embankment on soft subsoils

Authors Name: Jeevish Jindal, Prof Raju Sarkar

Dear Author,

With heartiest congratulations I am pleased to inform you that based on the recommendations of the reviewers and the Technical Program Committees, your paper identified above has been accepted for publication and oral presentation by **International Conference on Emerging Trends in Engineering , Science and Technology(ICEST-25)**

This conference received number of submissions from different countries and regions, reviewed by international experts and your paper cleared all the criteria, got accepted for the conference. Your paper will be published in the conference proceeding after the registration.

For registration: <https://www.sfe.net.in/conf/registration.php?id=3346483>

Herewith, the conference committee sincerely invites you to come to present your paper at our conference.

Sincerely,




Dr. James Crusoe
President
Society for Education (SFE)

 +91 9677007228

 info@sfe.net.in

 www.sfe.net.in